7. Li D, Shimamura T, Ji H, Chen L, Haringsma HJ, et al. (2007) Bronchial and peripheral murine lung carcinomas induced by T790M-L858R mutant EGFR respond to HKI-272 and rapamycin combination therapy. Cancer Cell 12: 81–93.
8. Soda M, Takada S, Takeuchi K, Choi YL, Enomoto M, et al. (2008) A mouse model for EML4-ALK-positive lung cancer. Proc Natl Acad Sci U S A 105: 19893–19897.
9. Rikova K, Guo A, Zeng Q, Possemato A, Yu J, et al. (2007) Global survey of phosphotyrosine signaling identifies oncogenic kinases in lung cancer. Cell 131: 1190–1203.
10. Bergethon K, Shaw AT, Ou SH, Katayama R, Lovly CM, et al. (2012) ROS1 Rearrangements define a unique molecular class of lung cancers. J Clin Oncol 30: 863–870.
11. Takeuchi K, Soda M, Togashi Y, Suzuki R, Sakata S, et al. (2012) RET, ROS1 and ALK fusions in lung cancer. Nat Med. 18: 378–381.
12. Rimkunas VM, Crosby KE, Li D, Hu Y, Kelly ME, et al. (2012) Analysis of Receptor Tyrosine Kinase ROS1-Positive Tumors in Non-Small Cell Lung Cancer: Identification of a FIG-ROS1 Fusion. Clin Cancer Res 18: 4449–4457.
13. Seo JS, Ju YS, Lee WC, Shin JY, Lee JK, et al. (2012) The transcriptional landscape and mutational profile of lung adenocarcinoma. Genome Res 22: 2109–2119.
14. Davies KD, Le AT, Theodoro MF, Skokan MC, Aisner DL, et al. (2012) Identifying and Targeting ROS1 Gene Fusions in Non-Small Cell Lung Cancer. Clin Cancer Res 18: 4570–4579.
15. Govindan R, Ding L, Griffith M, Subramanian J, Dees ND, et al. (2012) Genomic landscape of non-small cell lung cancer in smokers and never-smokers. Cell 150: 1121–1134.
16. Yoshida A, Kohno T, Tsuta K, Wakai S, Arai Y, et al. (in press) ROS1-rearranged lung cancer: a clinicopathological and molecular study of 15 surgical cases. Am J Surg Path in press.
17. Maher CA, Kumar-Sinha C, Cao X, Kalyana-Sundaram S, Han B, et al. (2009) Transcriptome sequencing to detect gene fusions in cancer. Nature 458: 97–101.
18. Chishti AH, Kim AC, Marfatia SM, Lutchman M, Hanspal M, et al. (1998) The FERM domain: a unique module involved in the linkage of cytoplasmic proteins to the membrane. Trends Biochem Sci 23: 281–282.
19. Charest A, Kheifets V, Park J, Lane K, McMahon K, et al. (2003) Oncogenic targeting of an activated tyrosine kinase to the Golgi apparatus in a glioblastoma. Proc Natl Acad Sci U S A. 100: 916–921.
20. Mishra A, Weaver TE, Beck DC, Rothenberg ME (2001) Interleukin-5-mediated allergic airway inflammation inhibits the human surfactant protein C promoter in transgenic mice. J Biol Chem 276: 8453–8459.
21. Fehon RG, McClatchey AI, Bretscher A (2010) Organizing the cell cortex: the role of ERM proteins. Nat Rev Mol Cell Biol 11: 276–287.
22. Medves S, Demoulin JB (2012) Tyrosine kinase gene fusions in cancer: translating mechanisms into targeted therapies. J Cell Mol Med 16: 237–248.
23. Inamura K, Takeuchi K, Togashi Y, Hatano S, Ninomiya H, et al. (2009) EML4-ALK lung cancers are characterized by rare other mutations, a TTF-1 cell lineage, an acinar histology, and young onset. Mod Pathol 22: 508–515.
24. Mino-Kenudson M, Chirieac LR, Law K, Hornick JL, Lindeman N, et al. (2010) A novel, highly sensitive antibody allows for the routine detection of ALK-rearranged lung adenocarcinomas by standard immunohistochemistry. Clin Cancer Res 16: 1561–1571.
25. Yoshida A, Tsuta K, Nakamura H, Kohno T, Takahashi F, et al. (2011) Comprehensive histologic analysis of ALK-rearranged lung carcinomas. Am J Surg Pathol 35: 1226–1234.
26. Charest A, Lane K, McMahon K, Park J, Preisinger E, et al. (2003) Fusion of FIG to the receptor tyrosine kinase ROS in a glioblastoma with an interstitial del(6)(q21q21). Genes Chromosomes Cancer 37: 58–71.
27. Gu TL, Deng X, Huang F, Tucker M, Crosby K, et al. (2011) Survey of tyrosine kinase signaling reveals ROS kinase fusions in human cholangiocarcinoma. PLoS One 6: e15640.
28. Birch AH, Arcand SL, Oros KK, Rahimi K, Watters AK, et al. (2011) Chromosome 3 anomalies investigated by genome wide SNP analysis of benign, low malignant potential and low grade ovarian serous tumours. PLoS One 6: e28250.
29. Park BS, El-Deeb IM, Yoo KH, Oh CH, Cho SJ, et al. (2009) Design, synthesis and biological evaluation of new potent and highly selective ROS1-tyrosine kinase inhibitor. Bioorg Med Chem Lett 19: 4720–4723.
30. Totoki Y, Tatsuno K, Yamamoto S, Arai Y, Hosoda F, et al. (2011) High-resolution characterization of a hepatocellular carcinoma genome. Nat Genet 43: 464–469.
31. Nannya Y, Sanada M, Nakazaki K, Hosoya N, Wang L, et al. (2005) A robust algorithm for copy number detection using high-density oligonucleotide single nucleotide polymorphism genotyping arrays. Cancer Res 65: 6071–6079.
32. Yoshikawa D, Ojima H, Kokubu A, Ochiya T, Kasai S, et al. (2009) Vandetanib (ZD6474), an inhibitor of VEGFR and EGFR signaling, as a novel molecular-targeted therapy against cholangiocarcinoma. Br J Cancer 100: 1257–1266.

Non-invasive X-ray Micro-computed Tomographic Evaluation of Indomethacin on Urethane-induced Lung Carcinogenesis in Mice

TOSHIYA UENO[1,2], KATSUMI IMAIDA[3], MITSUYOSHI YOSHIMOTO[1], TAKUYA HAYAKAWA[1,2], MAMI TAKAHASHI[4], TOSHIO IMAI[4], AKINORI YANAKA[2,5], KOJI TSUTA[6], MASAMI KOMIYA[1], KEIJI WAKABAYASHI[1,7] and MICHIHIRO MUTOH[1]

[1]*Division of Cancer Prevention Research, National Cancer Center Research Institute, Tokyo, Japan;*
[2]*Faculty of Pharmaceutical Sciences, Tokyo University of Science, Noda-shi, Japan;*
[3]*Onco-Pathology, Department of Pathology and Host-Defense, Faculty of Medicine, Kagawa University, Kagawa, Japan;*
[4]*Central Animal Division, National Cancer Center Research Institute, Tokyo, Japan;*
[5]*Hitachi Medical Education and Research Center, Division of Clinical Medicine, Faculty of Medicine, University of Tsukuba Hospital, Ibaraki, Japan;*
[6]*Clinical Laboratory Division, National Cancer Center Hospital, Tokyo, Japan;*
[7]*Graduate School of Nutritional and Environmental Sciences, University of Shizuoka, Shizuoka, Japan*

Abstract. *Background: Lung cancer is the leading cause of cancer-related death worldwide. We previously reported that respiration-gated X-ray micro-computed tomography (micro-CT) is a useful tool for analyzing lung tumor development in animal models. Materials and Methods: Lung tumors were induced by a single intraperitoneal injection (250 mg/kg) of urethane in male A/J mice, followed by indomethacin treatment at 5 ppm in the diet. The mice were scanned by micro-CT every 4 weeks from 10 to 26 weeks after urethane administration. Results: Total incidence and multiplicity of lung tumors were not significantly reduced by indomethacin treatment, as compared with untreated mice. However, the incidence of adenocarcinoma tended to be reduced by indomethacin treatment. Moreover, the size of lung tumors, especially adenomas, was suppressed by indomethacin treatment. Micro-CT analysis revealed that indomethacin effectively suppressed tumor development after urethane treatment for 10 weeks. Conclusion: These findings indicate that indomethacin suppresses lung carcinogenesis in mice and micro-CT is a useful non-invasive imaging approach for evaluating the characteristics and suppression of lung tumors in mice treated with cancer chemopreventive agents.*

Correspondence to: Michihiro Mutoh, Division of Cancer Prevention Research, National Cancer Center Research Institute, 5-1-1 Tsukiji, Chuo-ku, Tokyo 104-0045, Japan. Tel +81 335422511 ext. 4351, Fax +81 335439305, e-mail: mimutoh@ncc.go.jp

Key Words: Indomethacin, micro-CT, lung carcinogenesis, urethane, A/J mouse.

Lung cancer is the leading cause of cancer-related death worldwide (1), and reducing tobacco use and exposure to environmental carcinogens are effective ways to prevent lung carcinogenesis. The recent development of high-resolution computed tomography is able to identify small nodules in the lungs, including focal ground-glass opacities, which need to be followed in cancer check-ups. Thus, development of effective methods for preventing lung carcinogenesis is an urgent task.

Non-steroidal anti-inflammatory drugs (NSAIDs), such as indomethacin and aspirin, are reported to be useful chemopreventive agents for colorectal cancer, as demonstrated by experimental, epidemiological and clinical studies (2-6). NSAIDs, including indomethacin have also been shown to be useful candidate chemopreventive agents for lung tumors (7, 8). It has already been reported that indomethacin reduces the number of urethane-induced lung tumors in A/J mice (9). Indomethacin is a conventional NSAID, which has long been clinically employed to target inflammation. The molecular mechanisms underlying its protective effects are considered to be mainly due to inhibition of the activity of cyclooxygenase-1 (COX-1) and COX-2, key enzymes of prostanoid synthesis (10).

We recently applied X-ray micro-computed tomography (micro-CT) to detect lung space occupied lesions (SOLs) induced by a single intraperitoneal injection (250 mg/kg

BW) of urethane in male A/J mice, from 10 to 30 weeks after exposure to the carcinogen, and provided evidence that micro-CT is a useful non-invasive imaging approach for evaluating the characteristics and growth of lung tumors in mice (11). Our results also indicated that tumors grew at markedly varying speeds, and reflect histopatholgical findings after autopsy. Furthermore, these results indicate that micro-CT is also useful for evaluating lung tumor regression, induced by cancer chemopreventive agents.

In the present study, pre-neoplastic and neoplastic lesions (hyperplasia, adenoma and adenocarcinoma) were induced in the lungs of male A/J mice by a single intraperitoneal injection of urethane with or without indomethacin treatment at 5 ppm in the diet to evaluate its chemopreventive effects. In addition, lung SOL development was monitored periodically using respiration-gated micro-CT.

Materials and Methods

Animals. A/J Jms Slc mice, 5-week-old males, were purchased from Japan SLC Inc. (Hamamatsu, Japan) and five mice each were housed in a plastic cage with wood chip bedding in an air-conditioned animal room maintained at 24±2°C and 60±5% relative humidity, with a 12 h light-dark cycle. Basal diet (AIN-76A; CLEA Japan, Inc., Japan) and water were available *ad libitum* throughout the experiment.

Experimental protocol for A/J mice treated with indomethacin. At 6 weeks of age, mice (n=9) were treated with a single intraperitoneal injection of urethane (250 mg/kg; Sigma, St Louis, MO, USA) in 0.9% NaCl saline. Control mice (n=5) were given a single saline intraperitoneal injection. At the same time administration of indomethecin was started. Indomethacin was purchased from Sigma Chemical Co. (St Louis, MO, USA) and well-mixed at concentrations of 5 ppm with the basal diet. The dosage of indomethacin was determined by a previous report and our experiment (9, 12). The mice were scanned by micro-CT every 4 weeks from 10 to 26 weeks after urethane or control vehicle (0.9% NaCl saline) injection. The experiments were conducted according to the Guidelines for Animal Experiments in the National Cancer Center of the Committee for Ethics of Animal Experimentation of the National Cancer Center.

Micro-CT scan procedure. All mice were anesthetized with isoflurane (Dainippon Sumitomo Pharmaceutical Co., Osaka, Japan) and maintained anesthesia was achieved with a mixture of isoflurane and room air delivered during the scanning with micro-CT. Each mouse was placed on its back on an animal bed for micro-CT scanning, banded across the chest area, and a sensor for detecting respiration was placed on the abdomen. The X-ray scanning time point was set at 1,200 ms after expiration.

For scanning, a new cone-beam micro-CT scanner (eXplore Locus; General Electric Healthcare, London, Ontario, Canada) was used. The scan parameters that are consistent with gated *in vivo* scan acquisition include: 80 kV peak, 450 μA, 400 ms per frame, 0.5 degree at angle of increment and 720 views. The measured in-air radiation at iso-center was 240 mGy. Three-dimensional images obtained from axial, sagittal, coronal and oblique micro-CT images were reconstructed using MicroView (General Electric Healthcare).

Table I. *Multiplicity of lung SOLs in A/J Mice Treated with or without Indomethacin Assessed by Micro-CT.*

Indomethacin (ppm)	No. of mice	No. of SOLs/mouse				
		10	14	18	22	26 weeks
0	9	4.2±2.2	5.6±2.2	8.8±2.2	9.1±2.7	10.0±3.0
5	9	3.9±2.3	5.8±2.2	7.1±2.4	7.6±2.6	8.3±3.2

Data are mean±SD. SOL, space occupied lesion.

Histopathological examination. The mice were sacrificed 26 weeks after urethane administration and major organs, liver, kidneys and spleen, were weighed before fixation in 10% buffered formalin. Lungs were inflated for this purpose and lung SOLs, detected by a stereoscopic microscope, were embedded in paraffin blocks and sectioned at 3 μm for placement on slides and staining with hematoxylin and eosin for histopathological evaluation. Lung SOLs were diagnosed according to the criteria of the "International Classification of Rodent Tumors, The Mouse" (13) by a pathologist.

Human lung tissue samples. A total of 23 lung tissue samples were obtained from patients who underwent lobectomy at the National Cancer Center Hospital from 2006 to 2008. The paraffin-embedded sample stocks were used for integrin immunohistochemical staining. The samples include normal lung tissue (n=1), atypical adenomatous hyperplasia (n=11) and localized tumors with a lepidic growth pattern and alveolar collapse (Noguchi type B, n=11) (14), which were diagnosed by a pathologist. The study protocol was approved by the Institutional Review Board of the National Cancer Center, Tokyo, Japan.

Immunohistochemical staining. The sections used for histopathological evaluation in mice and humans were also used for immunohistochemical examination with the avidin–biotin complex immunoperoxidase technique. Polyclonal goat anti-COX-2 antibody (M-20) and polyclonal rabbit anti-vascular endothelial growth factor (VEGF) antibody (Santa Cruz Biotechnology, Santa Cruz, CA, USA) at 1:100 dilution were used. As a secondary antibody, anti-goat IgG, biotinylated and absorbed with rat serum (Vector Laboratories, Burlingame, CA, USA), was employed at 1:200 dilution. Staining was performed using avidin–biotin reagents (Vectastain ABC reagents; Vector Laboratories), 3,3'-diaminobenzidine and hydrogen peroxide, and the sections were counterstained with hematoxylin to facilitate orientation. As negative controls, consecutive sections were immunostained without exposure to the primary antibody.

Statistical analysis. The significance of differences in the multiplicity of urethane-induced mouse lung SOLs was analyzed using the Student's *t*-test, and statistical analysis for the number of SOLs which had more than doubled in diameter was performed with the χ^2 test. Differences were considered to be statistically significant with *p*-values of less than 0.05.

Table II. *Incidence and multiplicity of lung SOLs in A/J mice treated with or without indomethacin, assessed histopathologically.*

Indomethacin (ppm)	No. of mice	Hyperplasias		Adenomas (Ad)		Adenocarcinomas (Ca)		Total SOLs	Ad+Ca
		Incidence	Multiplicity	Incidence	Multiplicity	Incidence	Multiplicity	Multiplicity	Multiplicity
0	9	9 (100)	4.0±2.1	9 (100)	5.4±2.1	4 (44)	0.9±1.2	10.3±2.6	6.3±2.6
5	9	9 (100)	3.1±2.8	9 (100)	5.3±2.3	1 (11)	0.1±0.3^{+}	8.6±3.7	5.4±2.4

Data are mean±SD. Numbers in parentheses are percentages of mice with urethane-induced lung SOLs. ^{+}p=0.08 *vs.* 0 ppm.

Results

Incidence and multiplicity of lung SOLs assessed by micro-CT and histopathological analysis. The lung SOLs induced by urethane were easily distinguished from surrounding tissues in the micro-CT images. Reconstructed three-dimensional images were useful to differentiate the masses (globular) and blood vessels (tube structure) in lungs, even though both have a similar X-ray absorption. The smallest detectable SOL was approximately 0.5 mm in diameter. The incidence of SOLs detected by micro-CT was 100%, (10-26 weeks after urethane treatment). The number of SOLs/mouse (multiplicity) detected by micro-CT increased from 10 to 26 weeks after urethane treatment, as shown in Table I. The multiplicity of lung SOLs at 26 weeks after urethane treatment was 10.0±3.0 (mean±SD). With indomethacin treatment, the multiplicity of lung SOLs, determined by micro-CT at the end of the experiment, was reduced by approximately 20% as compared with the untreated mice (Table I).

Table II shows the incidence and multiplicity of lung SOLs at the end of experimental period, as determined by histopathological analysis. The number of total SOLs (10.3±2.6) was similar to that detected by micro-CT. The incidence of hyperplasia (bronchiolo-alveolar hyperplasia) and adenoma (bronchiolo-alveolar adenoma) was 100%, and that of adenocarcinoma (bronchiolo-alveolar adenocarcinoma) was 44%. No spontaneous tumors were observed in the A/J mice without urethane treatment. The actual number of lung SOLs examined by histopathological analysis was: eight adenocarcinomas in the indomethacin-untreated group, and one adenocarcinoma in the indomethacin-treated group. Similar numbers of hyperplasia and adenoma were detected in both indomethacin-treated and untreated groups. The multiplicity of adenocarcinoma averaged 0.9 in the indomethacin-untreated mice, and tended to be reduced to 0.1 (p=0.08) in the indomethacin-treated mice (Table II).

Change of number of lung SOLs by periodic micro-CT analysis. Periodic micro-CT analysis of urethane-induced lung SOLs in living mice revealed that the total number of

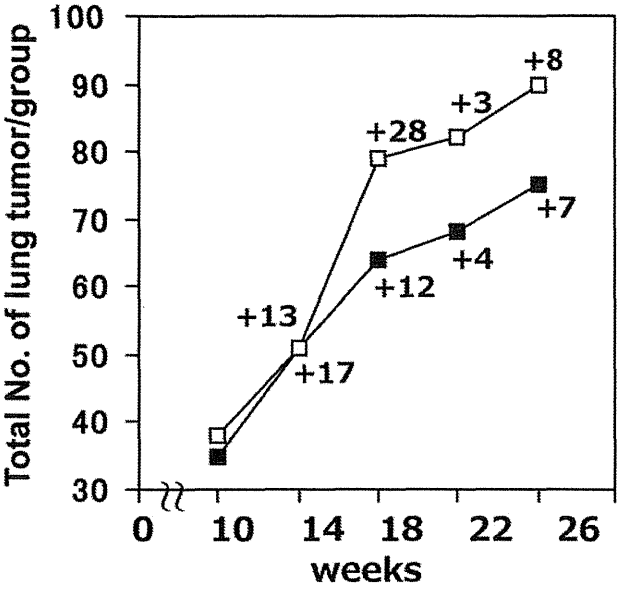

Figure 1. *Total number of lung space occupied lesions (SOLs) assessed by micro-computed tomography (CT). Increase of total lung SOLs from 10 to 26 weeks after urethane injection, detected by micro-CT, is shown. Open squares represent the control untreated group and closed squares indicate the indomethacin-treated group. The number of newly-detected SOLs in each group from 4 weeks is shown above or below the respective line.*

SOLs started to differ between groups from 18 weeks after urethane injection (Figure 1). Consistent with previous work (9), the percentage of reduction was almost the same throughout the experiment. Thus, the number of newly-developed SOLs within 4 weeks, *i.e.* newly-detected SOLs by micro-CT, in mice was counted successively, and are presented in Figure 1. Moreover, histopathological analysis revealed that tumors diagnosed as adenocarcinoma at the end of the experiment existed as SOLs in CT images from the early experimental periods: three tumors at 14 weeks and one tumor at 18 weeks. Interestingly, the number of newly-developed lung SOLs in the untreated group started to

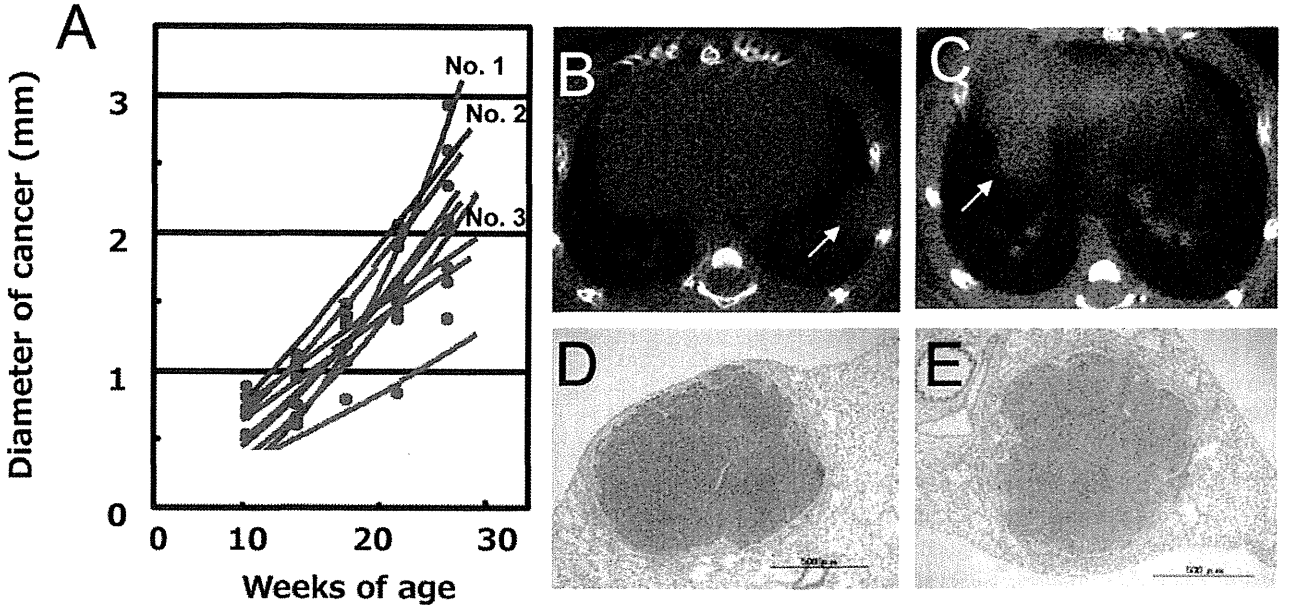

Figure 2. *Increase of lung adenocarcinoma diameters in A/J mice by axial micro-computed tomography (CT) images and histopathological hematoxylin and eosin (HE) staining. A: Growth curves of nine adenocarcinomas are shown. Each tumor scanned by micro-CT was reconstructed into three-dimensional images (axial, sagittal, coronal and oblique) and maximum diameters were measured periodically. The red line shows the growth of adenocarcinoma in the indomethacin-treated group. The blue line shows that of the untreated group. B: Micro-CT images of the most aggressive lung adenocarcinoma (curve no. 1 in A). C: Micro-CT images of lung adenocarcinoma in the indomethacin-treated group (curve no.2 in A). D: Histopathology of the lung space occupied lesion (SOL) shown in B. E: Histopathology of tumor shown in C. (D and E: bar=500 μm). Tumors observed in the lung are shown by arrows.*

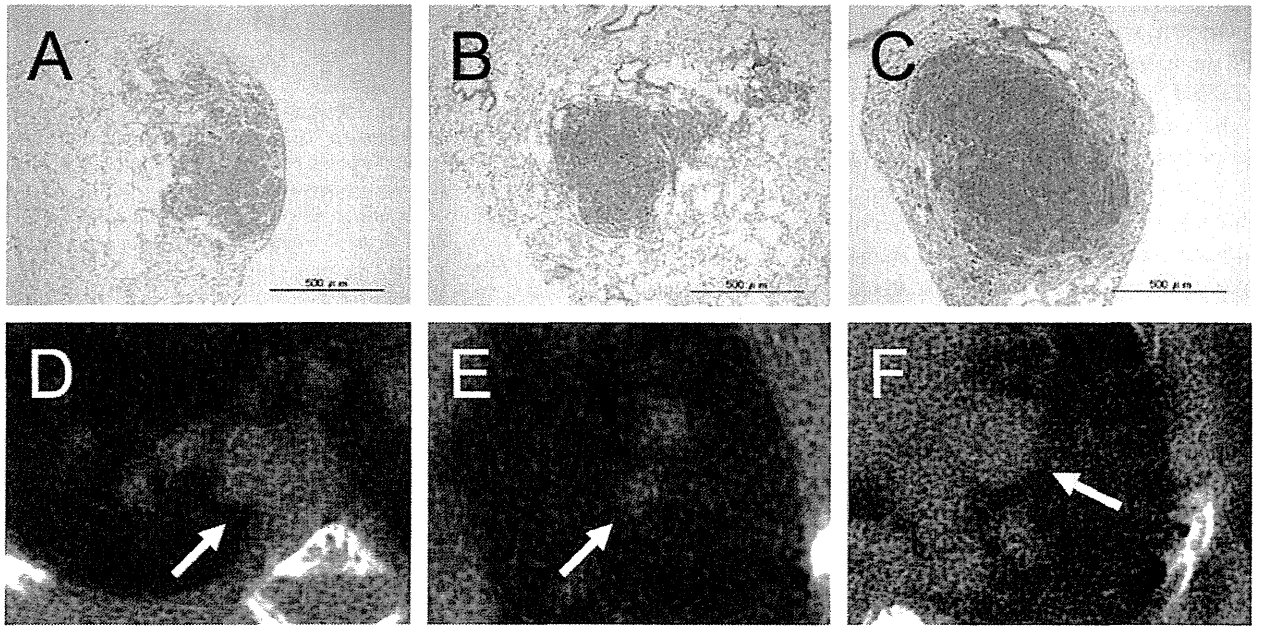

Figure 3. *Virtual in vivo micro-computed tomography (CT) images of lung space occupied lesion (SOL) and histopathological findings. Axial micro-CT images of the thorax of a mouse at the end of the experiment are shown. Histopathology of representative hyperplasia (A), adenoma (B) and adenocarcinoma (C) observed in urethane-treated mouse (all indomethacin-untreated mice); bar=500 μm. Micro-CT images representing hyperplasia (D), adenoma (E) and adenocarcinoma (F). Tumors observed in the lung are shown by arrows.*

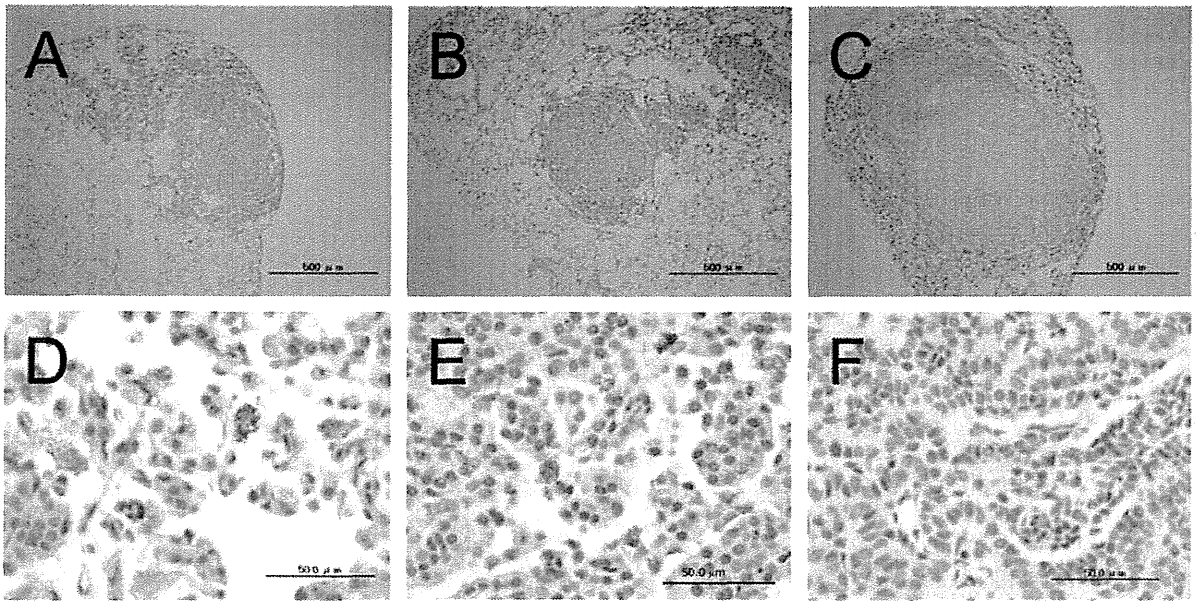

Figure 4. *Immunohistochemical findings for lung space occupied lesion (SOL) developed by urethane treatment. Immunohistochemical analysis of cyclooxygenase-2 (COX-2) (A-C) and vascular endothelial growth factor (VEGF) (D-F) expression in lung hyperplasia (A, D), adenoma (B, E) and adenocarcinoma (C, F) was performed using serial sections of the sample shown in Figure 3, respectively. Bar: 500 μm for A-C and 50 μm for D-F.*

Table III. *Size of lung SOLs at 26 weeks, assessed by micro-CT and by digital caliper.*

Indomethacin		Diameter (mm)				
		Hyperplasias	Adenomas (Ad)	Adenocarcinomas (Ca)	Total SOLs	Ad+Ca
0 ppm	Micro-CT	1.52±0.37	1.82±0.55	2.03±0.33	1.74±0.51	1.85±0.53
	Digital Caliper	1.42±0.55	1.79±0.56	1.94±0.65	1.65±0.60	1.81±0.58
5 ppm	Micro-CT	1.33±0.40	1.49±0.41 **	2.93	1.45±0.44 **	1.52±0.46**
	Digital Caliper	1.30±0.49	1.52±0.43*	2.65	1.46±0.48*	1.54±0.45*

Data are mean±SD. **p<0.01 *vs.* 0 ppm. *p<0.05 *vs.* 0 ppm.

decrease after 18 weeks, and indomethacin suppressed lung SOL development effectively at that period. Of note, one adenocarcinoma observed in the indomethacin-treated group, which was diagnosed at the end of experiment, existed as an SOL in CT images from 10 weeks.

Size of lung SOLs assessed by micro-CT. The longitudinal diameters of lung SOLs at 26 weeks, assessed by micro-CT, were similar to those measured by digital caliper after sacrifice (Table III). The longitudinal diameter tended to increase with histological changes, *i.e.* hyperplasia to adenocarcinoma. Indomethacin treatment reduced the size of lung tumors, especially of adenomas (Table III).

Figure 2A shows growth curves for all nine adenocarcinomas developed in A/J mice with or without indomethacin treatment. The adenocarcinoma grew most aggressively, 0.19 mm in diameter in one week (line no.1), and appeared as solid-type nodules with a clear tumor margin on micro-CT images (Figure 2B). Histopathologically, images exhibited an irregular nodular growth pattern without any glandular or tubular formation with little connective tissue. Nuclei were pleomorphic and mitotic figures were also observed (Figure 2D). Representative micro-CT images of hyperplasia, adenoma and other adenocarcinoma (line no.3 of Figure 2A) developed in A/J mice without indomethacin treatment, are shown in Figure 3. On the other hand, hyperplasia and adenoma grew at a slow to moderate speed throughout the experiment. These hyperplasias (Figure 3A) and adenomas (Figures 3B) exhibited clear edges and/or spiked edges in CT images. Figure 3B illustrates a papillary-type adenoma. As seen in adenoma, mitotic rates and degree of cellular pleomorphism were low. One adenocarcinoma

Table IV. *Number of lung SOLs grown more than twice in diameter in A/J mice assessed by micro-CT.*

Indomethacin	Hyperplasias	Adenomas (Ad)	Adenocarcinomas (Ca)	Total SOLs	Ad+Ca
0 ppm	12 (33)	32 (49)	8 (8)	52 (90)	31 (58)
5 ppm	10 (26)	18 (48)*	1 (1)	29 (75)*	18 (44)

Numbers in parentheses are total lung SOL numbers. *$p<0.05$ *vs.* 0 ppm.

(Figure 2A, red line, no.2), developed in the indomethacin-treated group was a large tumor that grew particularly rapidly, increasing from 0.9 mm to 2.9 mm within 16 weeks. This solid-type nodule with a clear tumor margin on CT images, is illustrated in Figure 2C.

The number of tumors that doubled in size from first detection was significantly reduced upon indomethacin treatment (Table IV). Regardless of indomethacin treatment, all adenocarcinomas more than doubled in diameter.

Expression of COX-2 and VEGF in lung SOLs. COX-2 immunostaining was performed to confirm the existence of molecules targeted by indomethacin (Figures 4A-C). The data were obtained from serial sections used for Figure 3. COX-2 was up-regulated in eight examined hyperplastic lesions. COX-2 was up-regulated in 10 out of 11 adenomas. Interestingly, COX-2 was down-regulated in all examined adenocarcinomas. Further details are summarized in Table V, in which COX-2 expression levels are classified into four groups (–, ±, + and ++) by staining strength. Moreover, VEGF immunostaining revealed that VEGF was observed in hyperplasia (6/8) and adenomas (8/11) but not in adenocarcinomas (Figures 4D-F).

COX-2 expression was also observed in macrophage and non-ciliated bronchiolar epithelial cells (clara cells) of human normal lung tissue, epithelial cells of atypical adenomatous hyperplasia and tumor cells of human lung tumors (Noguchi type B).

Table V. *Immunohistochemical analysis of COX-2 expression in lung SOLs without indomethacin treatment.*

Intensity	COX-2		
	Hyperplasias	Adenomas	Adenocarcinomas
–	0/8 (0)	1/11 (9)	4/10 (40)
±	0/8 (0)	3/11 (27)	1/10 (10)
+	5/8 (63)	5/11 (45)	0/10 (0)
++	3/8 (38)	2/11 (18)	0/10 (0)

–: Negative staining; ±: mixture lesion of – and +; +: positive staining; ++: strong-positive staining. Numbers in parentheses are percentages of mice with lung nodules.

Discussion

In the present study, micro-CT with a respiratory gating system was shown to be a useful non-invasive tool for evaluating the effects of indomethacin on urethane-induced lung SOL development in mice. This study provides evidence that indomethacin is able to suppress lung tumorigenesis at multiple stages, especially the adenoma-to-adenocarcinoma stage (Table II). Moreover, indomethacin treatment effectively suppressed the size of urethane-induced lung tumors (Table III).

In this urethane-induced lung tumor model, DNA mutations in lung epithelial cells are reported. Several tumor-susceptibility genes, such as cell-cycle-related genes (*Brca1*, *Cdkn2a/b*) and cell growth and angiogenesis-related genes (*Fos, Jun, Kras, Pkcn* and *Tnfa*) are mutated (15-20). Indomethacin has been reported to inhibit only the activity of β-catenin and COX, but not of cyclin-dependent kinase, activator protein 1 (AP-1) (Fos/Jun) and nuclear factor-kappa B (NF-κB) (21, 22). Thus, one can speculate that indomethacin inhibits lung tumor growth (Table IV) through direct inhibition of COX-1 and COX-2, which might be induced by *Fos, Jun, Kras, Pkcn* and *Tnfa* mutation.

Prostaglandin E_2 is reported to induce VEGF and increase the angiogenic response (23, 24). Moreover, indomethacin is reported to inhibit blood vessel formation in tumor-induced *in vivo* angiogenesis assays using C3H/HeJ mice (25). As shown in this study, expression of COX-2 was confirmed in hyperplasia and adenoma in the mice by immunohistochemical assay (Figure 4 and Table V). Expression of COX-2 was also confirmed in the early-stage of human lung tumors (Figure 5). Interestingly, COX-2 was down-regulated in adenocarcinoma, which might be the result of gene instability, as observed in the progressive stage of lung cancer (7). These data suggest that COX-2 inhibitor may be useful in preventing human lung tumor development. Furthermore, VEGF expression in adenoma may be related to the progression of adenoma to adenocarcinoma (Figure 4), and indomethacin may inhibit this angiogenic response.

Our data also propose candidate factors related to malignant transformation, including well-known factors. Proposed factors could be tumor size, tumor growth speed,

characteristics of nodules on CT image, and an allowed time span for tumor growth. Table III demonstrates the possibility that tumor size could correlate with histopathological type, but correlation seems weak. Tumor growth speed could be a strong candidate. However, our present and previous data showed that adenocarcinoma grew from slow to fast (Figure 2A), and we concluded that growth speed might be a susceptibility factor. Among the fast growing nodules, a smooth surface of the nodule (Figures 2B-E) is one of the characteristics of adenocarcinoma. The characteristics of lung adenocarcinoma in CT images need to be further investigated in detail. Finally, we concluded that the time span allowed for tumorigenesis is the most important factor for malignant transformation because our data (Figure 2B) demonstrate that all nodules which were finally diagnosed as adenocarcinoma at the end of the experiment existed at the early-stage of this experiment. These results indicate that the whole span of administration of indomethacin is not required to achieve similar chemopreventive effects of indomethacin, and experiments with several administration time spans are desired to obtain informative data.

In conclusion, our results provide evidence that respiratory-gated micro-CT scanning of live mice has the potential to evaluate the effects of cancer chemopreventive agents on lung tumorigenesis. Using this method, indomethacin revealed chemopreventive effects on lung tumorigenesis. Thus, this novel approach could be used as a screening technique for chemopreventive agents using a reduced number of sacrificed animals compared to other methods. Moreover, this novel approach may also have an impact on the study of natural lung tumor regression and of cancer therapeutic agents.

Acknowledgements

This work was supported by Grants-in-Aid for Cancer Research, for the Third-Term Comprehensive 10-Year Strategy for Cancer Control from the Ministry of Health, Labour and Welfare of Japan.

References

1 Jemal A, Murray T, Ward E, Samuels A, Tiwari RC, Ghafoor A, Feuer EJ and Thun MJ: Cancer statistics 2005. CA Cancer J Clin *55*: 10-30, 2005.

2 Thun MJ, Namboodiri MM and Heath CW Jr.: Aspirin use and reduced risk of fatal colon cancer. N Engl J Med *325*: 1593-1596, 1991.

3 Akasu T, Yokoyama T, Sugihara K, Fujita S, Moriya Y and Kakizoe T: Peroral sustained-release indomethacin treatment for rectal adenomas in familial adenomatous polyposis: A pilot study. Hepatogastroenterology *49*: 1259-1261, 2002.

4 Sandler RS, Halabi S, Baron JA, Budinger S, Paskett E, Keresztes R, Petrelli N, Pipas JM, Karp DD, Loprinzi CL, Steinbach G and Schilsky R: A randomized trial of aspirin to prevent colorectal adenomas in patients with previous colorectal cancer. N Engl J Med *348*: 883-890, 2003.

5 Baron JA, Cole BF, Sandler RS, Haile RW, Ahnen D, Bresalier R, McKeown-Eyssen G, Summers RW, Rothstein R, Burke CA, Snover DC, Church TR, Allen JI, Beach M, Beck GJ, Bond JH, Byers T, Greenberg ER, Mandel JS, Marcon N, Mott LA, Pearson L, Saibil F and van Stolk RU: A randomized trial of aspirin to prevent colorectal adenomas. N Engl J Med *348*: 891-899, 2003.

6 Reddy BS: Studies with the azoxymethane-rat preclinical model for assessing colon tumor development and chemoprevention. Environ Mol Mutagen *44*: 26-35, 2004.

7 Bauer AK, Malkinson AM and Kleeberger SR: Susceptibility to neoplastic and non-neoplastic pulmonary diseases in mice: genetic similarities. Am J Physiol Lung Cell Mol Physiol *287*: L685-703, 2004.

8 Moysich KB, Menezes RJ, Ronsani A, Swede H, Reid ME, Cummings KM, Falkner KL, Loewen GM and Bepler G: Regular aspirin use and lung cancer risk. BMC Cancer *2*: 31, 2002.

9 Moody TW, Leyton J, Zakowicz H, Hida T, Kang Y, Jakowlew S, You L, Ozbun L, Zia H, Youngberg J and Malkinson A: Indomethacin reduces lung adenoma number in A/J mice. Anticancer Res *21*: 1749-1755, 2001.

10 Vane JR, Bakhle YS and Botting RM: Cyclooxygenases 1 and 2. Annu Rev Pharmacol Toxicol *38*: 97-120, 1998.

11 Hori Y, Takasuka N, Mutoh M, Kitahashi T, Kojima S, Imaida K, Suzuki M, Kohara K, Yamamoto S, Moriyama N, Sugimura T and Wakabayashi K: Periodic analysis of urethane-induced pulmonary tumors in living A/J mice by respiration-gated X-ray microcomputed tomography. Cancer Sci *99*: 1774-1777, 2008.

12 Niho N, Mutoh M, Komiya M, Ohta T, Sugimura T and Wakabayashi K: Improvement of hyperlipidemia by indomethacin in Min mice. Int J Cancer *121*: 1665-1669, 2007.

13 Ulrich M: International Classification of Rodent Tumors: Mouse. New York: Springer-Verlag, 2001.

14 Noguchi M, Morikawa A, Kawasaki M, Matsuno Y, Hirohashi S, Kondo H and Shimosato Y: Small adenocarcinoma of the lung. Histologic characteristics and prognosis. Cancer *75*: 2844-2852, 1995.

15 Festing MF, Lin L, Devereux TR, Gao F, Yang A, Anna CH, White CM, Malkinson AM and You M: At least four loci and gender are associated with susceptibility to the chemical induction of lung adenomas in A/J x BALB/c mice. Genomics *53*: 129-136, 1998.

16 Gariboldi M, Manenti G, Canzian F, Falvella FS, Radice MT, Pierotti MA, Della Porta G, Binelli G and Dragani TA: A major susceptibility locus to murine lung carcinogenesis maps on chromosome 6. Nat Genet *3*: 132-136, 1993.

17 Manenti G, Gariboldi M, Elango R, Fiorino A, De Gregorio L, Falvella FS, Hunter K, Housman D, Pierotti MA and Dragani TA: Genetic mapping of a pulmonary adenoma resistance (*Par1*) in mouse. Nat Genet *12*: 455-457, 1996.

18 Pataer A, Nishimura M, Kamoto T, Ichioka K, Sato M and Hiai H: Genetic resistance to urethan-induced pulmonary adenomas in SMXA recombinant inbred mouse strains. Cancer Res *57*: 2904-2908, 1997.

19 Lin L, Festing MF, Devereux TR, Crist KA, Christiansen SC, Wang Y, Yang A, Svenson K, Paigen B, Malkinson AM and You M: Additional evidence that the *K-ras* protooncogene is a candidate for the major mouse pulmonary adenoma susceptibility (*Pas-1*) gene. Exp Lung Res *24*: 481-497, 1998.

20 Miyashita N and Moriwaki K: H-2-controlled genetic susceptibility to pulmonary adenomas induced by urethane and 4-nitroquinoline 1-oxide in A/Wy congenic strains. Jpn J Cancer Res *78*: 494-498, 1987.

21 Dihlmann S, Klein S and Doeberitz Mv MK: Reduction of beta-catenin/T-cell transcription factor signaling by aspirin and indomethacin is caused by an increased stabilization of phosphorylated beta-catenin. Mol Cancer Ther *2*: 509-516, 2003.

22 Tegeder I, Pfeilschifter J and Geisslinger G: Cyclooxygenase-independent actions of cyclooxygenase inhibitors. FASEB J *15*: 2057-2072, 2001.

23 Pai R, Szabo IL, Soreghan BA, Atay S, Kawanaka H and Tarnawski AS: PGE2 stimulates VEGF expression in endothelial cells *via* ERK2/JNK1 signaling pathways. Biochem Biophys Res Commun *286*: 923-928, 2001.

24 Uefuji K, Ichikura T and Mochizuki H: Cyclooxygenase-2 expression is related to prostaglandin biosynthesis and angiogenesis in human gastric cancer. Clin Cancer Res *6*: 135-138, 2000.

25 Rozic JG, Chakraborty C and Lala PK: Cyclooxygenase inhibitors retard murine mammary tumor progression by reducing tumor cell migration, invasiveness and angiogenesis. Int J Cancer *93*: 497-506, 2001.

Received August 13, 2012
Revised October 4, 2012
Accepted October 5, 2012

RESEARCH ARTICLE

Suppressive Effect of Pioglitazone, a PPAR Gamma Ligand, on Azoxymethane-induced Colon Aberrant Crypt Foci in KK-A^y Mice

Toshiya Ueno[1,3], Naoya Teraoka[1], Shinji Takasu[1], Katsuya Nakano[1,3], Mami Takahashi[2], Masafumi Yamamoto[2], Gen Fujii[1], Masami Komiya[1], Akinori Yanaka[3], Keiji Wakabayashi[4], Michihiro Mutoh[1]

Abstract

Obesity is an established risk factor for colorectal cancer. Pioglitazone is a peroxisome proliferator-activated receptorγ (PPARγ) agonist that induces differentiation in adipocytes and induces growth arrest and/or apoptosis *in vitro* in several cancer cell lines. In the present study, we investigated the effect of pioglitazone on the development of azoxymethane-induced colon aberrant crypt foci (ACF) in KK-A^y obesity and diabetes model mice, and tried to clarify mechanisms by which the PPARγ ligand inhibits ACF development. Administration of 800 ppm pioglitazone reduced the number of colon ACF / mouse to 30% of those in untreated mice and improved hypertrophic changes of adipocytes in KK-A^y mice with significant reduction of serum triglyceride and insulin levels. Moreover, mRNA levels of adipocytokines, such as leptin, monocyte chemoattractant protein-1 and plasminogen activator inhibitor-1, in the visceral fat were decreased. PCNA immunohistochemistry revealed that pioglitazone treatment suppressed cell proliferation in the colorectal epithelium with elevation of p27 and p53 gene expression. These results suggest that pioglitazone prevented obesity-associated colon carcinogenesis through improvement of dysregulated adipocytokine levels and high serum levels of triglyceride and insulin, and increase of p27 and p53 mRNA levels in the colorectal mucosa. These data indicate that pioglitazone warrants attention as a potential chemopreventive agent against obesity-associated colorectal cancer.

Key words: Pioglitazone - obesity - PPAR gamma - aberrant crypt foci

Asian Pacific J Cancer Prev, **13**, 4067-4073

Introduction

Colorectal cancer is one of the common cancers in developed countries including Japan. Many epidemiological studies have suggested colorectal cancer correlates with obesity, a high-fat diet and hyperlipidemia, especially, hypertriglyceridemia and high levels of low-density lipoprotein cholesterol (Le Marchand et al., 1997; Bruce et al., 2000). Assumed mechanisms underlying obesity-associated cancer development could involve insulin resistance, chronic inflammation and dyslipidemia caused by dysregulation of adipocytokine production. Among adipocytokines, increased levels of leptin, plasminogen activator inhibitor-1 (PAI-1), and decreased levels of adiponectin are demonstrated to play an important role in colorectal carcinogenesis (van Kruijsdijk et al., 2009).

Recently, we have reported that KK-A^y mice, carrying the Agouti yellow gene (A^y) and resultant hyperphagia (Nakamura et al., 1967), are highly susceptible to azoxymethane (AOM)-induced colorectal carcinogenesis (Teraoka et al., 2011). The KK-A^y mice exhibited severe abdominal obesity, hypertriglyceridemia and hyperinsulinemia. Moreover, serum pro-inflammatory adipocytokines such as interleukin-6 (IL-6), leptin and Pai-1 in KK-A^y mice were elevated and adiponectin was decreased compared to those in lean C57BL/6J mice. Among them, serum leptin levels were the highest in KK-A^y mice. Those features of KK-Ay mice could explain their high susceptibility to AOM-induced colorectal carcinogenesis, and suggests they could be useful to evaluate chemopreventive agents against obesity-associated colorectal cancer.

Peroxisome proliferator-activated receptorγ (PPARγ) is a key nuclear hormone receptor of lipid metabolisms and regulates several gene transcriptions associated with

*[1]Division of Cancer Prevention Research, [2]Central Animal Division, National Cancer Center Research Institute, Tokyo, [3]Faculty of Pharmaceutical Sciences, Tokyo University of Science, Chiba, [4]Graduate School of Integrated Pharmaceutical and Nutritional Sciences, University of Shizuoka, Shizuoka , Japan *For correspondence: mimutoh@ncc.go.jp*

differentiation, growth arrest and apoptosis (Fisher et al., 1998; Sporn et al., 2000). PPARγ directly activates lipoprotein lipase (LPL) promoter activity, and induces LPL, which catabolizes triglycerides to monoglycerides (Schoonjans et al., 1996). Activation of PPARγ also induces terminal differentiation of adipocytes linking to downsizing of hypertrophic adipotissue. Meanwhile, PPARγ induces growth arrest and apoptosis in several cancer cell lines, including colon, esophageal squamous, gastric and pancreatic cancer cells (Takahashi et al., 1999; Shimada et al., 2002; Rumi et al., 2002; Itami et al., 2001). Pioglitazone is a selective PPARγ agonist that improves hyperlipidemia and hyperglycemia in obese diabetic animals and humans (Sohda et al., 1990; Ikeda et al., 1990; Sakamoto et al., 2000). Although side effects, such as weight gain, peripheral edema, precipitation of chronic heart failure and an increase in bone fractures limit widespread use of pioglitazone, pioglitazone is a useful antidiabetic drug, which is well tolerated in the majority of patients (Shah et al., 2010). Previously, we have reported that pioglitazone induced LPL and suppressed concurrently both hyperlipidemia and intestinal polyp formation in *Apc*-deficient Min mice, a model mouse for familial adenomatous polyposis (Niho et al., 2003). Thus, pioglitazone may be a potential chemopreventive agent against colorectal carcinogenesis. Furthermore, pioglitazone may be a more useful chemopreventive agent against obesity-associated cancers, such as mammary cancer (Bojková et al., 2010).

In the present study, we investigated the effects of pioglitazone on the development of AOM-induced aberrant crypt foci (ACF) in obese KK-A^y mice. The novelty of this study is investigating the effect of pioglitazone in obese mice with retention of leptin and leptin receptor genes, in which we are able to examine actions of several molecules, such as adipocytokine, triglyceride and insulin with intact leptin signaling. The results demonstrated that pioglitazone prevented obesity-associated colorectal carcinogenesis through improving dysregulated levels of adipocytokines, especially leptin, insulin and lipids. Furthermore, another mechanism underlying the suppressive effect of pioglitazone is discussed with reference to induction of cell cycle-related genes.

Materials and Methods

Animals and chemicals

Female 5-week-old KK-A^y/TaJcl (KK-A^y) and C57BL/6J mice were purchased from CLEA Japan (Tokyo, Japan), and acclimated to laboratory conditions for 1 week. Five mice were housed per plastic cage with sterilized softwood chips as bedding in a barrier-sustained animal room at 24 ± 2°C and 55% humidity on a 12 hr light/dark cycle and fed AIN-76A powdered basal diet (CLEA Japan) and water. The animals in each cage were all in the same treatment group. The pioglitazone, {(±)-5-[4-[2-(5-ethyl-2-pyridyl)ethoxy] benzyl]thiazolidine-2,4-dione monohydrochloride}, was kindly provided by Takeda Chemical Industries, Ltd. (Osaka, Japan).

Experimental protocol for KK-A^y mice treated with azoxymethane and pioglitazone

For the induction of ACF by AOM (Nard Institute, Ltd., Amagasaki, Japan), 6-week-old female KK-A^y (n=10) were given intraperitoneal injections of AOM (200 μg/mouse) in 0.9% NaCl saline once a week for 3 weeks. Five mice were also injected with saline as a control group. At the same time of first intraperitoneal injections, pioglitazone was administrated at concentrations of 400 or 800 ppm in basal diet. The dosage of pioglitazone was determined by our previous experiment (Niho et al., 2003). Food and water were available ad libitum. The animals were observed daily for clinical signs and mortality. Body weights and food and water consumption were measured weekly. All the mice were anesthetized with ether and sacrificed at the age of 13 weeks, the organs, including intestinal tract, heart, kidneys, liver, lungs, spleen and visceral fat, were excised and were also observed macroscopically and blood samples from the caudal vena cava were collected. A part of visceral adipose tissue and liver tissue of KK-A^y mice with and without AOM treatment, and colon mucosa of KK-A^y mice without AOM treatment were rapidly deep-frozen in liquid nitrogen and stored at -80°C for further experiments. The experiments were performed according to the "Guidelines for Animal Experiments in the National Cancer Center" and were approved by the Institutional Ethics Review Committee for Animal Experimentation in the National Cancer Center.

Assessment of AOM-induced colorectal ACF

The intestinal tract was removed, the colorectum opened longitudinally and fixed flat between sheets of filter paper in 10% buffered formalin. After dividing the colorectum into the proximal segment and rectum (1.5 cm in length), halves of the remainder were divided into the middle and distal segment. These were stained with 0.2% methylene blue (Merck, Darmstadt, Germany) and the mucosal surface was assessed for ACF with a stereoscopic microscope, as previously reported (Bird et al., 1987).

Analysis of visceral adiposity

The images of visceral and subcutaneous fat were obtained by a cone-beam micro-CT scanner (eXplore Locus, General Electric Healthcare, Ontario, Canada) scanning from the first lumbar vertebra to the pubic bone. The volumes of the fat were analyzed by MicroView software (General Electric Healthcare).

Real-time polymerase chain reaction analysis

Total RNA was isolated from tissues by using Isogen (Nippon Gene, Tokyo, Japan), and treated with DNase I (Invitrogen, Carlsbad, CA, USA). One-μg RNA in a

Table 1. Development of Colorectal ACF in KK-A^y Mice Treated with AOM and Pioglitazone

Pioglitazone (ppm)	No. of mice with ACF	No. of ACF / colorectum					Mean no. of ACs / focus
		Proximal	Middle	Distal	Rectum	Total	
0	11 / 11	5.9 ± 3.3	19.1 ± 8.2	18.6 ± 5.2	6.9 ± 1.9	50.5 ± 13.9	1.6 ± 0.2
400	10 / 10	1.6 ± 2.6 **	6.5 ± 3.6 **	22.2 ± 9.3	9.7 ± 5.7	40.0 ± 13.4	1.4 ± 0.2
800	10 / 10	0.1 ± 0.3 **	3.8 ± 2.3 **	19.6 ± 6.2	8.4 ± 2.8	31.9 ± 6.6 *	1.5 ± 0.2

Data are means ± SD. *p<0.05, **p<0.01 vs 0 ppm

final volume of 20 μL was used for synthesis of cDNA using an Omniscript® RT Kit (Qiagen, Hilden, Germany) with an oligo (dT) primer. Real-time PCR was carried out using a DNA Engine OpticonTM 2 (MJ Japan Ltd., Tokyo, Japan) with SYBR Green Real-time PCR Master Mix (Toyobo Co., Osaka, Japan). Primers for mouse adiponectin (5'-AGGATGCTACTGTTGCAAGCTCTC, 3'- CAGTCAGTTGGTATCATGGTAGAG), GAPDH (5'- TTGTCTCCTGCGACTTCA, 3'- CACCACCCTGTTGCTGTA), IL-6 (5'- ACAACCACGGCCTTCCCTACTT, 3'- CACGATTTCCCAGAGAACATGTG), leptin (5'- CCAAAACCCTCATCAAGACC, 3'- GTCCAACTGTTGAAGAATGTCCC), LPL (5'- GGATCCGTGGCCGCAGCAGACGCAGGA, 3'- GAATTCCATCCAGTTGATGAATCTGGCCAC), monocyte chemoattractant protein (MCP-1) (5'- CCACTCACCTGCTGCTACTCAT, 3'- TGGTGATCCTCTTGTAGCTCTCC), Ob-Rbl (5' Primer- CCATCTTTTATATGATCTGCCTGAAGT, 3' Primer- TGCATTGGACAGTCTGAAAGCT), Pai-1 (5'- ACAGCCTTTGTCATCTCAGCC, 3'- AGGGTTGCACTAAACATGTCAG), tumor necrosis factor-a(TNF-a) (5'- TGTGCTCAGAGCTTTCAACAAC, 3'- GCCCATTTGAGTCCTTGATG), p27 (5'- TCTCAGGCAAACTCTGAGGA, 3'- CTTCCTCATCCCTGGACACT), p53 (5'- CCCCAGGATGTTGAGGAGTTT, 3'- TTGAGAAGGGACAAAAGATGACA) were employed (Teraoka et al., 2011; Niho et al., 2005; Turmelle et al., 2006; Xiao et al., 2009). To assess the specificity of each primer set, amplicons generated from the PCR reaction were analyzed for melting curves.

Measurement for serum lipids, adipocytokine and insulin

Serum levels of triglycerides and total cholesterol were measured as reported (Niho et al., 2003). Serum levels of adiponectin, interleukin-1β (IL-1β), IL-6, MCP-1, leptin and insulin were measured using mouse adiponectin immunoassay (R&D systems, Inc., Minneapolis, MN, USA), mouse procarta® cytokine assay (Affymetrix, Inc., Santa Clara, CA, USA), a mouse leptin enzyme-linked immunosorbent assay kit (B-Bridge International, Inc., Cupertino, CA, USA) and a mouse insulin kit (Millipore Corp., Billerica, MA, USA).

Immunohistochemical analysis

The colon (segment of middle and distal) after analysis of colon ACF formation and the liver and the visceral fat were sliced and processed to sections stained with hematoxylin and eosin (H&E). Sections of middle and distal colon were also stained immunohistochemically with antibodies against proliferation cell nuclear antigen (PCNA; DAKO, Carpinteria, CA, USA) used at 200 x dilution. The number of PCNA positive cells was measured in a crypt from three different arbitrarily selected points in colon mucosa (n=5). The extent of enlargement of adipocytes was evaluated by quantification of the number of adipocyte nuclei observed in the field (x 200) of fat tissue in KK-A^y mice.

Statistical analysis

The significance of difference in the number of AOM-induced colorectal ACF, serum lipid levels and serum cytokine levels was analyzed using Dunnett's multiple comparison test and other statistical analyses were performed with Student's t-test. Differences were considered to be statistically significant at $p<0.05$.

Results

Suppression of the numbers of AOM-induced colorectal ACF in KK-Ay mice by pioglitazone

To determine the effect of pioglitazone on colorectal ACF development in obese KK-A^y mice, KK-A^y mice were treated with AOM and pioglitazone. Administration of pioglitazone did not significantly effect food intake, behavior or body weight changes during the experiment periods. Final body weights in 13-week-old female KK-A^y mice untreated, treated with 400 ppm pioglitazone and 800 ppm pioglitazone were 45.7 ± 3.1 (mean ± SD), 40.0 ± 3.4 and 42.0 ± 3.5 g, respectively.

Table 1 shows data for the numbers and distribution of colorectal ACF in KK-A^y mice with or without pioglitazone. All KK-Ay mice treated with AOM developed ACF in the colorectum at 13 weeks. The total numbers of ACF in the groups treated with pioglitazone at 400 and 800 ppm doses were reduced to 79 and 63 % ($p<0.05$) of the control value, respectively. Of note, the number of ACF in the proximal and middle parts of the colon in the mice fed diet containing 400 and 800 ppm pioglitazone were reduced significantly ($p<0.01$). There were no significant differences in the mean numbers of ACs per focus among each group.

Improvement of fatty change in the liver and hypertrophy of adipocytes in the visceral fat tissue by pioglitazone

To clarify the effects of AOM and pioglitazone on other tissue, histopathological examination were

Table 2. Amount of Fat Tissue in KK-*Ay* Mice Treated with AOM and Pioglitazone

Pioglitazone (ppm)	Visceral fat (g)	Subcutaneous fat (g)	Total (g)
0	6.2 ± 0.9	2.0 ± 0.4	8.2 ± 1.2
800	4.2 ± 0.4 **	1.6 ± 0.1 *	5.9 ± 0.5 **

Data are means ± SD. *p<0.05, **p<0.01 vs 0 ppm; Amount of fat tissue was analyzed by micro-CT

Table 3. Levels of Serum Lipids and Insulin in KK-*Ay* Mice Treated with AOM and Pioglitazone

Pioglitazone (ppm)	Triglycerides (mg / dL)	Total cholesterol (mg / dL)	Insulin (ng / mL)
0	502.0 ± 128.4	103.8 ± 19.3	39.5 ± 2.8
400	262.8 ± 81.2**	89.7 ± 10.9	3.5 ± 1.6**
800	254.3 ± 62.3 **	97.7 ± 16.8	4.4 ± 3.5 **

Data are means ± SD. **p<0.01 vs 0 ppm

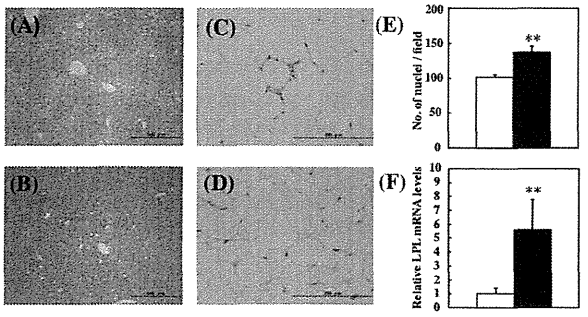

Figure 1. Fatty Change in the Liver and Size of Adipocytes in the Visceral Fat Tissue. (A, B) Representative histopathological sections (H&E) of the liver in KK-*Ay* mice and the liver of the mice treated with 800 ppm pioglitazone are shown, respectively. (C, D) Representative histopathological sections (H&E) of the visceral fat in KK-*Ay* mice and the mice treated with 800 ppm pioglitazone, respectively. (E) Numbers of nuclei of visceral fat cells in a microscopical field were counted and are shown. (F) Hepatic LPL mRNA expression levels were examined by real-time PCR analysis. GAPDH mRNA was used to normalize the data. Values were set at 1.0 in untreated control Data are means ± SE (n=5). **, p<0.01.

performed on the liver and visceral fat tissue. The weights of liver at the end of experiments in KK-*Ay* mice treated with AOM and 0, 400 and 800 ppm pioglitazone treated group were 1.7 ± 0.1 (mean ± SD), 1.7 ± 0.2 and 1.9 ± 0.2 g, respectively. As shown in Figure 1A, fatty change of the liver was observed in KK-*Ay* mice by histopathological examination, and was clearly improved by administration of 800 ppm pioglitazone (Figure 1B).

The volume of visceral and subcutaneous fat was measured by a micro-CT, and these amounts are summarized in Table 2. Treatment with 800 ppm pioglitazone in KK-*Ay* mice significantly decreased the amount of visceral fat (p<0.01), subcutaneous fat (p<0.05) and total fat (p<0.01) compared with those of the untreated control. The amounts of mesenteric fat tissue in KK-*Ay* mice untreated, treated with 400 ppm and 800 ppm pioglitazone were 1.5 ± 0.4 (mean ± SD), 0.7 ± 0.2 (p<0.01 vs 0 ppm) and 0.7 ± 0.3 g (p<0.01 vs 0 ppm), respectively. Histopathological examination of visceral adipose tissue clearly showed that the size of adipocytes in visceral adipose tissue in KK-*Ay* mice treated with 800 ppm pioglitazone was smaller than that in untreated control mice (Figure 1C and 1D). Moreover, the number of adipocyte nuclei observed in one field of visceral fat tissue under the microscope (x200) in KK-*Ay* mice was 101.0 ± 10.0, and treatment with 800 ppm pioglitazone significantly increased the number to 137.0 ± 20.0 (p<0.01) (Figure 1E).

Improvement of the levels of lipids, insulin and adipocytokines in serum of KK-Ay mice treated with pioglitazone

To evaluate the effects of pioglitazone on the size reduction of adipocytes in the visceral fat tissue, the levels of serum lipids, insulin and adipocytokines were measured, and are summarized in Tables 3 and 4. The average serum levels of triglycerides and insulin, but not total cholesterol of KK-*Ay* mice treated with AOM and 400 ppm or 800 ppm pioglitazone were significantly decreased compared with those of KK-*Ay* mice treated AOM alone (Table 3). Thus, we investigated the effects of pioglitazone on hepatic mRNA levels of LPL,

Table 4. Levels of Serum Adipocytokines in KK-*Ay* Mice Treated with AOM and Pioglitazone

Pioglitazone (ppm)	Adiponectin (mg / mL)	IL-1β (pg / mL)	IL-6 (pg / mL)	MCP-1 (pg / mL)	Leptin (ng / mL)
0	12.7 ± 1.5	54.1 ± 17.6	26.4 ± 20.4	155.1 ± 37.2	140 ± 31.7
400	14.5 ± 0.9	36.6 ± 6.80*	12.2 ± 2.60	138.6 ± 26.9	45.9 ± 27.2**
800	27.9 ± 2.0 **	51.4 ± 10.7	35.0 ± 20.8	99.3 ± 36.1**	46.5 ± 21.7 **

Data are means ± SD. **p<0.01 vs 0 ppm, . *p<0.05 vs 0 ppm

Table 5. PCNA Immunostaining in Middle or Distal Colon of KK-*Ay* Mice Treated with AOM and 800 ppm Pioglitazone

Pioglitazone (ppm)	Cells / crypt		PCNA positive cell / crypt		% of PCNA positive cells / total cells crypt	
	Middle	Distal	Middle	Distal	Middle	Distal
0	42.0 ± 4.2	39.6 ± 3.3	17.0 ± 4.7	12.2 ± 2.7	41.2 ± 11.4	30.6 ± 7.0
800	38.6 ± 3.5	34.2 ± 3.9	12.9 ± 2.7	12.1 ± 2.7	33.4 ± 5.8	35.8 ± 8.8

Data are means ± SD

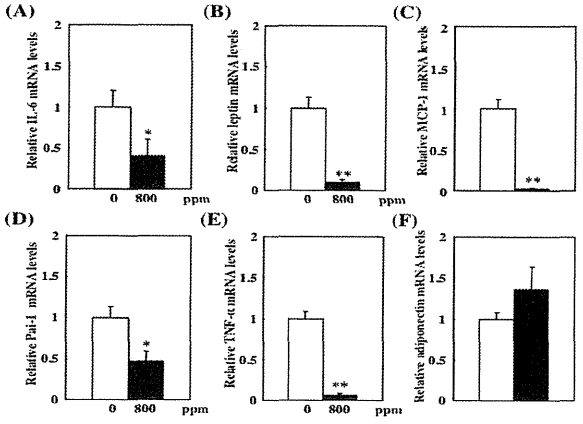

Figure 2. Relative Expression Levels of Adipocytokine mRNA in Visceral Fat Tissue of KK-Ay Mice. Real-time PCR analysis was performed to obtain IL-6 (A), leptin (B), MCP-1 (C), Pai-1 (D), TNF-α (E) and adiponectin (F) mRNA expression levels. GAPDH mRNA was used to normalize the data. White, untreated control group. Black, 800 ppm pioglitazone treated group. Values were set at 1.0 in the untreated control. Data are means ± SE (n=5). *, p<0.05, **, p<0.01.

which catabolizes triglycerides to monoglycerides. Administration of 800 ppm pioglitazone increased 5.6-fold the hepatic LPL mRNA levels compared with those of untreated control levels (Figure 1F). The serum adiponectin level was also significantly increased and serum levels of leptin and MCP-1 were significantly decreased in KK-Ay mice treated with 800 ppm pioglitazone compared with untreated KK-A^y mice ($p<0.01$). Significant differences were also obtained in serum levels of IL-1β and leptin in KK-A^y mice treated with 400 ppm pioglitazone (Table 4).

Improvement of the levels of adipocytokines in visceral fat tissue of KK-Ay mice treated with pioglitazone

Data for the mRNA expression levels of adipocytokines in visceral fat tissue are shown in Figure 2. The mRNA expression levels of IL-6, leptin, MCP-1, Pai-1 and TNF-α in KK-A^y mice treated with AOM and 800 ppm pioglitazone were significantly decreased compared with those of KK-Ay mice treated with AOM alone. On the other hand, treatment of 800 ppm pioglitazone had a tendency to up-regulate the mRNA expression of adiponectin compared with untreated KK-A^y mice.

Validation of colon epithelial cell proliferation in KK-Ay mice treated with pioglitazone and/or AOM

To investigate the effect of pioglitazone treatment on epithelial cell proliferation of colon mucosa in KK-A^y mice, the amount of cells in S phase and expression of cell cycle-related gene (p27 and p53) were examined. PCNA immunohistochemical staining revealed that administration of 800 ppm pioglitazone had a tendency to suppress cell proliferation in the colon mucosa in KK-A^y mice. As shown in Table 5, the total cells per crypt in middle colon mucosa of KK-A^y mice and the mice treated with 800 ppm pioglitazone were 41.2 ± 11.4 and 33.4 ± 5.8, and PCNA positive cells in those mice were 17.0 ± 4.7 and 12.9 ± 2.7, respectively. In distal colon mucosa, the number of PCNA positive cells was almost the same between the each group. Related to cell proliferation, leptin elicits its biological activity through Ob-Rbl, and downstream targets, Akt, Erk and STAT3, may stimulate cell growth signaling with modifying cell cycle-related genes. Thus we examined cell cycle-related genes, p27 and p53. The treatment with 800 ppm pioglitazone up-regulated the mRNA levels of p27 ($p<0.05$) and p53 ($p<0.05$), and down-regulated leptin receptor Ob-Rbl ($p<0.05$) in the colorectal mucosa of KK-Ay mice without AOM compared with that of untreated control mucosa (Figure 3).

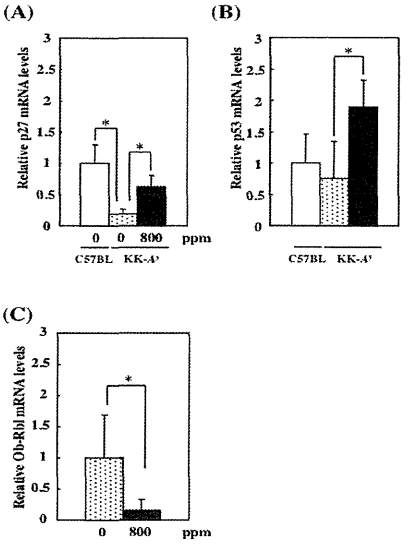

Figure 3. Relative Expression Levels of Cell Cycle-related Genes and Leptin Receptor in Colorectal Mucosa of KK-Ay Mice and C57BL/6J Mice. Real-time PCR analysis was performed to obtain p27 (A), p53 (B) and Ob-Rbl (C) mRNA expression levels. GAPDH mRNA was used to normalize the data. White, untreated control C57BL/6J mice. Dotted, untreated KK-Ay mice. Black, 800 ppm pioglitazone treated KK-Ay mice. Values were set at 1.0 in untreated control. Data are means ± SE (n=4). *, p<0.05.

Discussion

In the present study, pioglitazone treatment decreased the number of AOM-induced ACF in obese KK-A^y mice. This suppressive effect of pioglitazone might be explained by involvement of systemic improvement of dysregulated adipocytokine, triglyceride and insulin levels, and increase of mRNA levels of p27 and p53 in the colorectal mucosa of KK-A^y mice. This study provided the evidence that pioglitazone could be a useful chemopreventive agent against obesity-associated colorectal cancer.

It has been reported that hypertrophic change of adipocytes evokes dysregulated adipocytokine production (Cowey et al., 2006; van Kruijsdijk et al., 2009). Thus, we examined the size of adipocytes in visceral adipose tissue in KK-A^y mice treated with pioglitazone and found the

size to be much smaller than those in untreated control mice. These data are consistent with previous reports that PPARγ, a member of the nuclear receptor superfamily, stimulated preadipocyte differentiation, and reduced the size of adipocytes to the normal size (Schoonjans et al., 1996). Size reduction of adipocyte is suggested to improve insulin resistance along with reduced serum triglyceride levels. In fact, serum levels of triglycerides, insulin and leptin levels were decreased at a dose of 800 ppm pioglitazone, and serum adiponectin was increased. In addition, the expression of LPL was increased in the liver being related to reduction of serum triglyceride levels. It has been reported that the PPAR-responsible elements exist in the promoter region of the LPL gene, and indeed, pioglitazone increased hepatic expression levels of LPL. Moreover, the mRNA expression levels of IL-6, leptin, MCP-1, Pai-1 and TNF-α in visceral adipose were reduced by pioglitazone treatment, and adiponectin tended to be increased in the present study. It has been reported that PPARγ ligand inhibits Ob-Rbl mRNA expression in human hepatic stellate cells (Schoonjans et al., 1996). Several experiments using thiazolidinediones, selective ligands of PPARγ, revealed that PPARγ targets adiponectin, IL-6, MCP-1 and TNF-α and increase adiponectin expression levels but decrease the rest (Iwaki et al., 2003).

The expression of cell cycle-related genes (p27 and p53) in colorectal mucosa of KK-A^y mice was down-regulated compared with those of C57BL/6J mice, which are generally used as non-obese, non-diabetic controls (Figure 3). P27 and p53, which belong to the Cip/Kip family of cyclin-dependent kinase inhibitors, play a key role in cell growth arrest (Polyak et al., 1994). The administration of 800 ppm pioglitazone increased the expression levels of low p27 and p53 mRNA levels observed in the colorectal mucosa of KK-A^y mice. Leptin elicits its biological activity through Ob-Rbl, and downstream targets, Akt, Erk and STAT3, may stimulate cell growth signaling with modifying cell cycle-related genes. It has been reported that STAT3 would play both a positive regulatory role and a negative one for p27 expression (Fukada et al., 1998; Kortylewski et al., 1999). Thus, it is implicated that low p27 and p53 in the obese mice could be due to high serum levels of leptin in part, and that increased expression of p27 and p53 by pioglitazone treatment could due to a decrease of leptin expression. Of note, insulin and insulin-like growth factors are strong growth factors modifying cell cycle-related genes and may affect colorectal ACF development. The serum level of insulin, drastically decreased with pioglitazone, also could explain the effects of pioglitazone on ACF development. The ratio of contribution of the factors, such as adipocytokine, insulin and triglyceride should be revealed in the future.

It is interesting that pioglitazone suppressed AOM-induced ACF development in the upper portion of the colorectum (proximal and middle colon), but not lower portion (distal colon and rectum). To clarify the localized specific effect of pioglitazone, PCNA immunohistochemical staining was conducted in middle and distal colon. As a result, administration of 800 ppm pioglitazone had a tendency to reduce PCNA positive cells in the middle colon in KK-A^y mice. Moreover, there were no significant differences in mRNA levels of p27 and p53 between the middle and distal parts (data not shown). Comparing the numbers of ACF in AOM-treated lean C57BL/6J mice with those of KK-A^y mice, KK-A^y mice increased the number of ACF in the proximal and middle colon (Teraoka et al., 2011). However, the effect of pioglitazone on different portions of the colon in obese mice could not be explained. Further examinations with novel aspects are needed to clarify the different action of pioglitazone on ACF development in the distal and middle colon.

In conclusion, pioglitazone has a potential benefit to suppress AOM-induced ACF development in obese KK-A^y mice in a systematic and direct manner. Pioglitazone also could effectively suppress intestinal polyp development in Min mice (Niho et al., 2003). Thus, pioglitazone might be a good candidate for a chemopreventive agent against obesity-associated colorectal cancer. Meanwhile, a cohort study showed no clear associations between use of pioglitazone and reduced risk of colon cancer incidence in diabetes patients (Ferrara et al., 2011), with the limitation of short periods of follow up, less than 6 years, after the initiation of pioglitazone. Thus, further epidemiological studies with long periods of follow up are desired to evaluate pioglitazone, as a potential chemopreventative agent in humans.

Acknowledgement

This work was supported by Grants-in-Aid for Cancer Research, for the Third-Term Comprehensive 10-Year Strategy for Cancer Control from the Ministry of Health, Labour, and Welfare of Japan, and also from the Yakult Bio-science Foundation. S.T. was the recipient of a Research Resident Fellowship from the Foundation for Promotion of Cancer Research.

References

Bird RP (1987). Observation and quantification of aberrant crypts in the murine colon treated with a colon carcinogen: preliminary findings. *Cancer Letts*, **37**, 147-51.

Bojková B, Garajová M, Kajo K, et al (2010). Pioglitazone in chemically induced mammary carcinogenesis in rats. *Eur J Cancer Prev*, **19**, 379-84.

Bruce WR, Wolever TM, Giacca A (2000). Mechanisms linking diet and colorectal cancer: the possible role of insulin resistance. *Nutr Cancer*, **37**, 19-26.

Cowey S, Hardy RW (2006). The metabolic syndrome: A high-risk state for cancer? *Am J Pathol*, **169**, 1505-22.

Ferrara A, Lewis JD, Quesenberry CP Jr, et al (2011). Cohort study of pioglitazone and cancer incidence in patients with diabetes. *Diabetes Care*, **34**, 923-9.

Fisher B, Costantino JP, Wickerham DL, et al (1998). Tamoxifen for prevention of breast cancer: report of the national surgical adjuvant breast and bowel project P-1 study. *J Natl Cancer Inst*, **90**, 1371-88.

Fukada T, Ohtani T, Yoshida Y, et al (1998). STAT3 orchestrates contradictory signals in cytokine-induced G1 to S cell-cycle transition. *EMBO J*, **17**, 6670-7.

Ikeda H, Taketomi S, Sugiyama Y, et al (1990). Effects of pioglitazone on glucose and lipid metabolism in normal and insulin resistant animals. *Arzneimittelforschung*, **40**, 156–62.

Itami A, Watanabe G, Shimada-Itami A, et al (2001). Ligands for peroxisome proliferator-activated receptorγ inhibit growth of pancreatic cancers both in vitro and in vivo. *Int J Cancer*, **94**, 370–6.

Iwaki M, Matsuda M, Maeda N, et al (2003). Induction of adiponectin, a fat-derived antidiabetic and antiatherogenic factor, by nuclear receptors. *Diabetes*, **52**, 1655-63.

Kortylewski M, Heinrich PC, Mackiewicz A, et al (1999). Interleukin-6 and oncostatin M-induced growth inhibition of human A375 melanoma cells is STAT-dependent and involves upregulation of the cyclin-dependent kinase inhibitor p27/Kip1. *Oncogene*, **18**, 3742-53.

Le Marchand L, Wilkens LR, Kolonel LN, et al (1997). Association of sedentary lifestyle, obesity, smoking, alcohol use, and diabetes with the risk of colorectal cancer. *Cancer Res*, **57**, 4787-94.

Nakamura M, Yamada K (1967). Studies on a diabetic (KK) strain of the mouse. *Diabetologia*, **3**, 212-21.

Niho N, Mutoh M, Takahashi M, et al (2005). Concurrent suppression of hyperlipidemia and intestinal polyp formation by NO-1886, increasing lipoprotein lipase activity in Min mice. *Proc Natl Acad Sci USA*, **102**, 2970-4.

Niho N, Takahashi M, Shoji Y, et al (2003). Dose-dependent suppression of hyperlipidemia and intestinal polyp formation in Min mice by pioglitazone, a PPARγ ligand. *Cancer Sci*, **94**, 960-64.

Polyak K, Kato JY, Solomon MJ, et al (1994). p27Kip1, a cyclin-Cdk inhibitor, links transforming growth factor-beta and contact inhibition to cell cycle arrest. *Genes Dev*, **8**, 9-22.

Rumi MA, Sato H, Ishihara S, et al (2002). Growth inhibition of esophageal squamous carcinoma cells by peroxisome proliferator-activated receptor γ ligands. *J Lab Clin Med*, **140**, 17–26.

Sakamoto J, Kimura H, Moriyama S, et al (2000). Activation of human peroxisome proliferator-activated receptor (PPAR) subtypes by pioglitazone. *Biochem Biophys Res Commun*, **278**, 704–11.

Schoonjans K, Peinado-Onsurbe J, Lefebvre AM, et al (1996). PPARalpha and PPARgammma activators direct a distinct tissue-specific transcriptional response via a PPRE in the lipoprotein lipase gene. *EMBO J*, **15**, 5336-48.

Schoonjans K, Staels B, Auwerx J (1996). The peroxisome proliferator activated receptors (PPARs) and their effects on lipid metabolism and adipocyte differentiation. *Biochim Biophys Acta*, **1302**, 93-109.

Shah P, Mudaliar S (2010). Pioglitazone: side effect and safety profile. *Expert Opin Drug Saf*, **9**, 347-54.

Shimada T, Kojima K, Yoshiura K, et al (2002). Characteristics of the peroxisome proliferators activated receptor gamma (PPAR gamma) ligand induced apoptosis in colon cancer cells. *Gut*, **50**, 658-64.

Sohda T, Momose Y, Meguro K, et al (1990). Studies on antidiabetic agents. Synthesis of hypoglycemic activity of 5-[4-(pyridylalkoxy)benzyl]-2,4-thiazolidinediones. *Arzneimittelforschung*, **40**, 37–42.

Sporn MB, Suh N (2000). Chemoprevention of cancer. *Carcinogenesis*, **21**, 525-30.

Takahashi N, Okumura T, Motomura W, et al (1999). Activation of PPARγ inhibits cell growth and induces apoptosis in human gastric cancer cells. *FEBS Lett*, **455**, 135-9.

Teraoka N, Mutoh M, Takasu S, et al (2011). High susceptibility to azoxymethane-induced colorectal carcinogenesis in obese KK-Ay Mice. *Int J Cancer*, **102**, 79-87.

Turmelle YP, Shikapwashya O, Tu S, et al (2006). Rosiglitazone inhibits mouse liver regeneration. *FASEB J*, **20**, 2609-11.

van Kruijsdijk RC, van der Wall E, Visseren FL (2009). Obesity and cancer: the role of dysfunctional adipose tissue. *Cancer Epidemiol Biomarkers Prev*, **18**, 2569-78.

Xiao X, Wang Y, Gong H, et al (2009). Molecular evidence of senescence in corneal endothelial cells of senescence-accelerated mice. *Mol Vis*, **15**, 747-61.

Cancer Letters 334 (2013) 56–61

Contents lists available at SciVerse ScienceDirect

Cancer Letters

journal homepage: www.elsevier.com/locate/canlet

Mini-review

Metabolic syndrome: A novel high-risk state for colorectal cancer

Kousuke Ishino [a], Michihiro Mutoh [b], Yukari Totsuka [a], Hitoshi Nakagama [a,b,*]

[a] Division of Cancer Development System, National Cancer Center Research Institute, 5-1-1 Tsukiji, Chuo-ku, Tokyo 104-0045, Japan
[b] Division of Cancer Prevention Research, National Cancer Center Research Institute, 5-1-1 Tsukiji, Chuo-ku, Tokyo 104-0045, Japan

ARTICLE INFO

Keywords:
Metabolic syndrome
Colon carcinogenesis
Advanced glycation end products

ABSTRACT

Metabolic syndrome (MS) and related disorders, including cancer, are steadily increasing in most countries of the world. However, mechanisms underlying the link between MS and colon carcinogenesis have yet to be fully elucidated. In this review article we focus on the relationships between various individual associated conditions (obesity, dyslipidemia, diabetes mellitus type 2 and hypertension) and colon cancer development, and demonstrate probable related factors revealed by *in vivo* and *in vitro* studies. Furthermore, molecules suggested to be involved in cancer promotion are addressed, and the potential for cancer prevention by targeting these molecules is discussed.

1. Introduction

Many disorders can be induced by excessive accumulation of visceral adipose tissue, and the combination of related symptoms, so-called metabolic syndrome (MS), is attracting increasing attention as a major health problem since it can lead to conditions such as cardiovascular disease. Recently, MS has also attracted much interest as a risk factor for several cancers, including colon cancer. The World Cancer Research Fund and American Institute for Cancer Research have evaluated causal relationships between accumulation of visceral adipose tissue and cancer, and concluded 'confident evidence' for colorectum and pancreas cancers [1]. In Japan, overweight and obesity, defined as a body mass index (BMI) of 25 or more, are similarly reported to be associated with several cancers, such as colorectum cancer in males, breast cancer in postmenopausal females and liver cancer in those with a history of hepatitis C virus infection [2–4].

In this review article, relationships between the symptoms of MS and colorectal carcinogenesis are focused on in animal models. Commonly used animals for MS models are rodents because of their size. The models are classified into three groups: diet-induced obesity models (C57BL/6J mice and F344 rats), monogenic models (*ob/ob* mice, *db/db* mice, ZDF rats and KK-A^y mice), and polygenic models (TSOD mice and OLETEF rats). A high-fat/-fructose diet, or mice with genetic alterations such as mutation of leptin, leptin receptor and agouti genes are commonly used. Suitable animal models of MS-associated carcinogenesis might be mice with intact leptin and leptin receptors because leptin signaling stimulates cell growth, and may affect carcinogenesis.

2. Metabolic syndrome

MS is common in Western countries, and is currently increasing almost ubiquitously across the globe. In addition to developed countries, MS is increasing in developing countries in adults and particularly in children [5]. Moreover, obesity and overweight are rapidly increasing in both urban and rural areas in the under developed countries of sub-Saharan Africa and South Asia [6].

Various diagnostic criteria for MS have been proposed by many national/international organizations [7–10]. Consensus statements for diagnosis of MS are almost the same, and these are the presence of any three abnormal findings out of five. i.e. (1) waist circumference (males: $\geqslant$90 cm; females: $\geqslant$80 cm), (2) blood triglyceride (TG) levels $\geqslant$150 mg/dL (1.7 mmol/L), (3) blood high-density lipoprotein (HDL) cholesterol levels (males < 40 mg/dL (1 mmol/L); females <50 mg/dL (1.3 mmol/L), (4) blood pressure (systolic blood pressure $\geqslant$130 mmHg and/or diastolic blood pressure $\geqslant$85 mmHg or drug treatment for hypertension), and (5) blood sugar (fasting blood sugar $\geqslant$100 mg/dL (5.6 mmol/L) or drug treatment for diabetes mellitus type 2 (T2DM)) [11]. However, further work is required for the components regarding waist circumference, which rely on population and country-specific definitions [12].

A major pathogenesis of this syndrome could be accumulation of visceral adipose tissue, characterized by increased numbers of macrophage infiltration along with low-grade inflammation [13]. In addition to low-grade inflammation, other factors that may contribute to colorectal cancer development would be dyslipidemia, insulin resistance, subsequent adipocytokine imbalance and activation of the renin-angiotensin system, which are further documented in detail in this paper Fig. 1.

* Corresponding author. Address: Division of Cancer Prevention Research, National Cancer, Center Research Institute, 5-1-1 Tsukiji, Chuo-ku, Tokyo 104-0045, Japan.
E-mail address: hnakagam@ncc.go.jp (H. Nakagama).

0304-3835/$ - see front matter © 2012 Elsevier Ireland Ltd. All rights reserved.
http://dx.doi.org/10.1016/j.canlet.2012.10.012

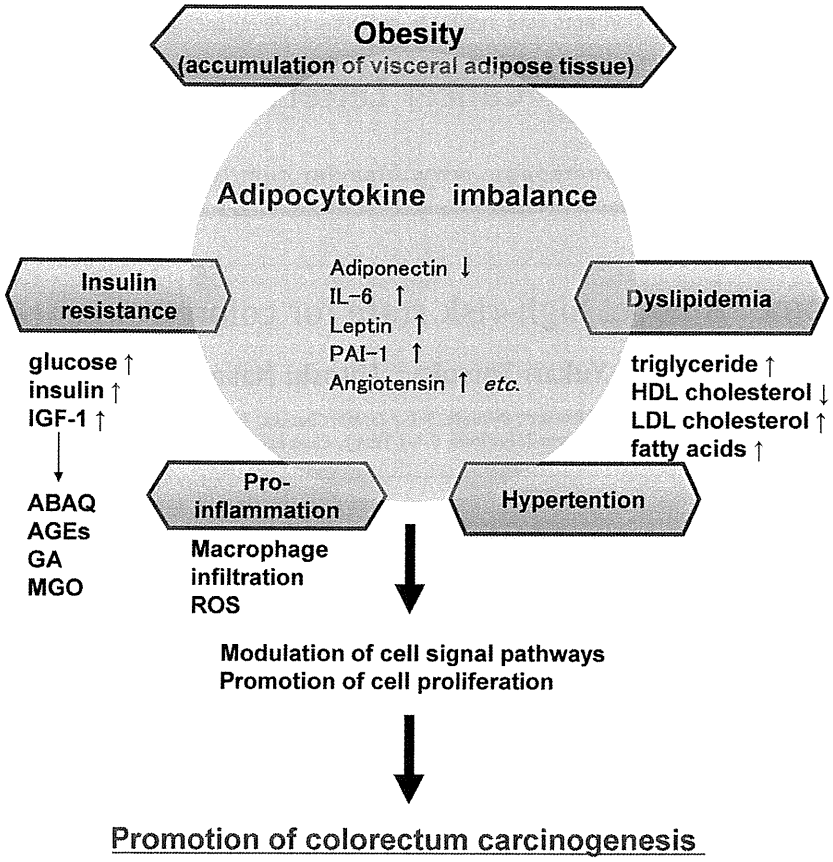

Fig. 1. Assumed relationship between metabolic syndrome and imbalance of adipocytokine production linked to colorectal cancer development. AGEs, advanced glycation end products; GA, glyceraldehydes; HDL, high-density lipoprotein; IGF-1, insulin like growth factor-1; IL-6, interleukine-6; LDL, low-dencity lipoprotein; MGO, methylglyoxal; PAI-1, plasminogen activator inhibitor-1; ROS, reactive oxygen species.

3. Dyslipidemia

Hypertriglyceridemia is associated with an elevated risk (HR = 1.71) of colon cancer in Japanese men [14]. In the case of a precursor lesion of colorectal cancer, most epidemiological studies have consistently showed that serum TG levels are associated with their increase [15–18]. Thus, it is considered that serum TG, lipoprotein lipase (LPL), a key enzyme that catalyzes the hydrolysis of TG, could play important roles in carcinogenesis.

In animal models of human familial adenomatous polyposis (FAP), *Apc*^{1309} (C57BL/6J$^{Apc/ApcD1309}$) [19] and *Min* mice [20,21], elevated serum TG has been observed with suppression of mRNA levels for LPL in the liver and small intestine. Although no significant differences were observed between *Apc*^{1309} mice and wild-type mice at 6 weeks of age, the average serum TG value in *Apc*^{1309} mice at 12 weeks was found to be markedly increased almost 10-fold (~600 mg/dL) as compared to that at 6 weeks. A similar increase of TG levels (almost 400 mg/dL) was observed in *Min* mice at 15 weeks compared to the 8 weeks time point.

The anti-T2DM agent, pioglitazone, is a potent peroxisome proliferater-acitivated receptor γ (PPAR γ) ligand with a weak binding affinity for PPARα. PPAR responsive elements exist in the promoter region of the *LPL* gene, and pioglitazone has been confirmed to increase LPL mRNA levels in the liver and intestinal epithelial cells in *Apc*-deficient mice. Serum levels of TG at 12 weeks of the *Apc*^{1309} mice were reduced to 44% and 50% by 100 and 200 ppm of pioglitazone treatment, respectively, with a 33% decrease in the total numbers of polyps (Table 1) [19]. *Min* mice treated with 100–1600 ppm pioglitazone for 14 weeks also showed a decrease of intestinal polyps to 63–9% of the control number [20]. Administration of 100 and 200 ppm bezafibrate, a PPAR α ligand, which also elevates LPL mRNA, to *Apc*^{1309} mice reduced serum levels of TG dose dependently up to 55% ($P < 0.05$), with a reduction in the total numbers of polyps by 13% and 25% ($P < 0.05$), respectively [20]. We further treated *Min* mice with the LPL selective inducer NO-1886, demonstrated to possess no PPAR agonistic activity, unlike bezafibrate or pioglitazone [22,23], and showed 400 and 800 ppm doses to significantly decrease the total number of intestinal polyps to 48% and 42%, respectively, of the untreated control value, in mice (Table 1) [24]. Of note, NO-1886 caused a marked increase in *LPL* mRNA levels in the liver and the small intestine [24]. Based on these results, suppression of serum TG levels by increasing LPL activity is suggested to contribute to a reduction of intestinal polyp formation under *Apc*-deficient conditions, and both TG and LPL could be good molecular targets for colon cancer prevention.

Table 1
Summary of tumor suppressive effects of chemopreventive agents.

Agent	Dose (ppm)	Mouse model	Suppression to the untreated control group (%)	Refs.
Pioglitazone	200	*Apc*^{1309}	67	[48]
Pioglitazone	1600	Min	9	[49]
Bezafibrate	200	*Apc*^{1309}	75	[49]
NO-1886	800	Min	42	[53]
SK-216	100	Min	56	[42]

4. Diabetes

Insulin resistance is characteristic of metabolic syndrome, associated with high levels of fasting glucose, insulin and insulin-like

Table 2
Representative dicarbonyl compounds: occurrence and consequent mutations.

Compound[a]	Mutation spectrum	Target base	Increase in diabetic patients[b]
MGO	G:C → T:A [41] G:C → C:G	G, A [34]	3.5-fold [32]
GO	G:C → T:A [42] G:C → C:G	G, A, C [35]	2.2-fold [32]
GA	Unknown	G [36]	2-fold [38][c]

[a] Abbreviations: MGO, methylglyoxal; GO, glyoxal; GA, glyceraldehyde.
[b] Compared with healthy control.
[c] Detected as amino acid adducts.

growth factor (IGF-1) in the blood. It is considered that these conditions are linked to T2DM, and a higher risk of colon cancer [25,26]. For example, hyperglycemia, hyperinsulinemia and high level of IGF-1 have been demonstrated to increase cell viability and proliferation observed in an *in vitro* setting [27].

Multiple genetic alterations in tumor-related genes have been identified in various types of cancers [28]. With obesity or under T2DM conditions, an increased level of reactive oxygen species (ROS) has been reported in multiple sites, such as blood, liver and adipose tissue. In animal experiments, Furukawa et al. demonstrated that production of ROS in adipose tissue increased body weight-dependently, and ROS production was stimulated by fatty acids *via* NADPH oxidase activation [29]. Moreover, there have been several reports of significantly elevated oxidative DNA damage in blood of T2DM patients [30]. ROS attack of nucleotide bases in DNA yields a variety of alterations and damaged nucleosides that escape repair have the capacity to introduce mutations during DNA replication [31]. Based on these findings, T2DM may contribute to induction of mutations and colon carcinogenesis *via* increased oxidative stress.

In diabetes (both type 1 and type 2) patients, glucose concentrations in blood are at high levels compared with healthy subjects all day long. It has been reported that reduced sugars, including glucose, are non-enzymatically converted into dicarbonyl compounds, such as methylglyoxal (MGO), glyceraldehyde (GA), under physiological conditions [32]. Such dicarbonyl compounds react irreversibly with amino groups of physiological components, such as protein, DNA and lipid by the Maillard reaction, to form glycation adducts or so-called Advanced Glycation End products (AGEs) [33–36]. These have been detected as amino acid- [37,38], deoxyribonucleoside (nucleobase)- [39] and phospholipid-adducts [40], in both types of diabetic patients. Glycation products of DNA are known to induce mutations in mammalian [41,42] and bacterial cells [43], such as, for example, G:C to C:G and G:C to T:A transversions in the *supF* gene in simian kidney cells associated with N^2-(1-carboxyethyl)-2′-deoxyguanosine produced by the reaction of 2′-deoxyguanosine with MGO (Table 2) [41].

Furthermore, we discovered a novel Maillard reaction product formed from L-tryptophan and glucose, 5-amino-6-hydroxy-8*H*-benzo[6,7]azepino[5,4,3-de]quinolin-7-one, ABAQ, showing mutagenicity toward various Salmonella strains in the presence of S9 mix [44]. Because of a consistent increase in blood glucose levels under T2DM conditions its production might be enhanced in T2DM individuals. We are now investigating the presence of ABAQ *in vivo* using urine samples collected from DM rat models and DM patients.

5. ROS and inflammation

As mentioned in the previous section, DNA damage induced by ROS is likely to play an important role in carcinogenesis, and obesity increases ROS levels in adipose tissue and blood. In MS patients, abdominal fat tissue attracts macrophages by induction of several chemokines, such as monocyte chemoattractant protein-1 (MCP-1), and forms crown-like structures [13]. Activated macrophages are known to produce ROS and inflammatory cytokines, and thus obesity is now considered to be a pro-inflammatory condition.

ROS directly effects cell proliferation and apoptosis through modification of gene expression followed by activation of transcription factors, such as members of the AP-1 and NF-κB pathways [45]. Activation of AP-1 results in induction of cyclin D1, which in turn promotes entry into mitosis, while NF-κB induces inflammatory cytokines and growth factors, which enhance the inflammation status. A recent report demonstrated that ROS and prostaglandin E_2, which play important roles in inflammation in colon cancer tissue, modulate DNA methylation patterns [46], control gene expression and may thereby contribute to the multistage carcinogenesis process.

Lipid peroxidation mediated by ROS has also been recognized to play a key role in carcinogenesis, for example by activation of transcriptional factors [47]. Free and ester forms of unsaturated fatty acids and cholesterol are easily attacked by ROS, and are oxidized by a chain mechanism. Colorectal cancer risk in a case-control study showed positive relationships with erythrocyte membrane compositions of palmitic and oleic acids, but negative links with linoleic ($18:2n-6$) and arachidonic acids [48]. *Min* mice with a hyperlipidemic state demonstrate elevated values for palmitic and oleic acids in plasma and erythrocyte membranes, and higher plasma levels of linoleic acid, indicating these to be important in intestinal polyp formation [49]. In addition, detailed analysis of serum lipids in *Min* mice using reverse-phase liquid chromatography/electrospray ionization mass spectrometry revealed that hydroperoxidizable TG precursors containing linoleic acid were deposited at the tips of villi with aging, and these hydroperoxidized TG were also increased in serum [50]. Such increases of oxidizable TG precursors in serum and small intestinal mucosa could be reduced by treatment with pitavastatin, a novel lipophilic statin [50], with concomitant reduction of intestinal polyp development [51]. These results indicated that quantitative and qualitative lipid changes affect the course of intestinal polyp formation in *Min* mice, and support the idea that oxidative stress might lead to the development of colon cancer.

6. Adipocytokine imbalance

Obese mice, such as the KK-A^y strain, are highly susceptible to induction of colon premalignant lesions, aberrant crypt foci (ACF), and development of colorectal carcinomas on exposure to azoxymethane (AOM) [52]. KK-A^y mice were established by crossmating KK, T2DM model mice, with C57BL/6J-A^y mice [53,54], which carry the *Agouti* gene (*Ay*), and feature severe hyperphagia, hyperinsulinemia and dyslipidemia. C57BL/6J mice are generally used as non-obese controls [55,56]. The numbers of AOM-induced ACF per mouse and tumor per mouse developing in KK-A^y mice (almost 70 and 8, respectively) also appeared higher than in other obese mice, *ob/ob* or *db/db* mice, not possessing intact leptin or leptin receptors [52]. In addition to severe hyperinsulinemia and hypertriglyceridemia, the KK-A^y mouse exhibits abdominal obesity, and resultant elevation of serum adipocytokines, such as interleukin-6 (IL-6), leptin and plasminogen activator inhibitor-1 (Pai-1) compared with values for lean C57BL/6J mice. In the visceral fat tissue, significant over-expression of pro-inflammatory adipocytokine mRNAs such as for IL-6, leptin, MCP-1, Pai-1 and tumor necrosis factor (TNF)-α were confirmed; in contrast, that for adiponectin was decreased. The consequent adipocytokine imbalance is suggested to be involved in the promotion of colon carcinogenesis.

Our recent findings for two adipocytokines, adiponectin and PAI-1, and their relevance to intestinal tumorigenesis provide

further support for this idea. Adiponectin is a 30 kDa protein, present at high levels in plasma (range, 3–30 μg/mL), inversely correlated with the BMI [57,58]. Moreover, low plasma adiponectin levels are associated with insulin resistance, high serum glucose levels, and coronary artery disease [59–61] as well as with increased risk of various cancers, including colorectal cancer [62,63].

Thus, we investigated how low levels of adiponectin might be involved in colon carcinogenesis using *Min* mice. Adiponectin-deficient *Min* mice of both sexes exhibited a 2- or 3-fold increase in the total number of intestinal polyps compared to those of adiponectin-wild *Min* mice at the ages of 9 and 12 weeks [64]. In addition, adiponectin-deficient C57BL/6 J mice treated with AOM showed increased incidences and multiplicities of colorectal adenomas and adenocarcinomas. AMPKα activation through the adiponectin receptor, AdipoR1, inhibits Akt activation followed by mammalian target of rapamycin (mTOR) inactivation [63,65], presumably through abolished signaling from AdipoR1, enhancing cell growth and tumor development.

In primary cell culture, fibroblasts from adiponectin-deficient C57BL/6J mice over-express Bcl-2 compared to those of adiponectin-wild C57BL/6J mice [64,66]. Adiponectin deficiency also affects production of other adipocytokines. Adiponectin-deficient *Min* mice exhibit an increase in serum Pai-1 levels with adiponectin gene dosage [64], in agreement with the tendency for elevation observed with adiponectin-deficiency at the age of 55 weeks in C57BL/6J mice [64]. Treatment with an AMPK activator, metformin, was also found to lower amounts of hepatic Pai-1 mRNA in *Min* mice, in line with earlier reports [67,68]. Thus, it is conceivable that Pai-1 levels are generally depressed by adiponectin.

PAI-1, a serine protease inhibitor (serpin) protein, which inhibits the function of tissue plasminogen activator and urokinase-type plasminogen activator by direct binding, demonstrates increased levels with obesity and the metabolic syndrome. PAI-1 can be induced by TG, very low-density lipoprotein, transforming growth factor β (TGFβ) and various growth factors [69–72]. There is also evidence that the serum PAI-1 concentration may be a reliable indicator of a poor prognosis in colorectal cancer [73–79].

In our experiments, serum Pai-1 levels in the 15-week-old male *Min* mice could be shown to be 8 times higher than in wild-type mice, while hepatic Pai-1 mRNA levels were 11-fold increased. Administration of a PAI-1 inhibitor, SK-216, at 25, 50 and 100 ppm doses in the diet for 9 weeks reduced serum Pai-1 levels and hepatic Pai-1 mRNA levels of *Min* mice compared to the wild-type levels. Moreover, *Min* mice receiving SK-216 at 50 and 100 ppm exhibited significantly reduced total numbers of intestinal polyps, to 64% and 56% of the untreated group value, respectively (Table 1). Serum TG levels were also decreased by 43% at the dose of 100 ppm [80]. These results indicate that Pai-1 induction associated with hypertriglyceridemia may contribute to intestinal polyp formation with *Apc* deficiency. Thus, adiponectin and PAI-1 are considered to be key molecules involved in obesity-associated cancers.

7. Angiotensin-renin system

Activation of the renin–angiotensin system (RAS) has been implicated in the etiology of hypertension, obesity and metabolic syndrome [81]. Angiotensin II (Ang II) elicits its biological activities through two well-defined receptors, type 1 (AT1R) and type 2 (AT2R), to elevate blood pressure, and agents that block AT1R, angiotensin-converting enzyme (ACE) activity and calcium influx block such elevation. It is not clear whether hypertension affects neoplasia, but accumulating evidence suggests that activation of RAS is involved in development of various cancers, such as in the breasts, colorectum, kidneys and lungs [82].

AT1R expressed in a wide variety of tissues activates downstream MAPK and STAT signal pathways [83]. Thus, Ang II- AT1R -mediated signals induce expression of protooncogenes such as *c-fos*, *c-myc* and *c-jun*, and thereby promote cell proliferation [84,85]. In animal models, the AT1R blockers (ARBs) captopril and telmisartan have been shown to suppress the development of ACF and more advanced preneoplastic lesions, β-catenin accumulated crypts, in male *db/db* obese mice [86]. Moreover, captopril or telmisartan decreased the mRNA levels of TNF-α, COX-2, IL-1β, IL-6, and PAI-1 in the white adipose tissue of AOM-treated *db/db* mice.

ACE inhibitors block the formation of Ang II and have been demonstrated to attenuate tumor growth in experimental animals [87–90] and to reduce the risk of several human cancers [91]. AT2R expression is low in adult tissues, although detectable in heart, kidneys, pancreas, adrenal glands, uterus, ovaries and brain [92], and AT2R-mediated signals counteract AT1R-mediated actions [82,93]. It is interesting that down-regulation of cytochrome P450 2E1 expression in the liver of AT2R-null mice resulted in an increase in the number of AOM-induced colon tumors [94]. Calcium blockers are also primarily utilized to control peripheral blood pressure. Some of them, such as verapamil, are known to inhibit p-glycoprotein (encoded by *Mdr1a* gene), and the number of polyps in *Min* mice undergoing verapamil administration was significantly decreased [95].

The available findings with anti-hypertensive agents appear clinically significant because these drugs are widely used for patients with hypertension who frequently are obese. Inhibition of RAS might be an effective strategy for prevention of colon cancer.

8. Future aspects

Understanding the molecules involved in obesity-associated cancer may provide clues to cancer preventive strategies in obese individuals. There appears to be a convergence of effects of dyslipidemia, insulin resistance, inflammation and adipocytokines. Targeting related molecules and signaling pathways may therefore be a good preventive and/or therapeutic approach. Some studies suggest that weight loss after gastric bypass surgery is associated with a reduced incidence of cancer [96]. Its ability to reduce the risk of obesity-associated cancers needs to be confirmed in future investigations. In addition, factors reducing the risk of obesity-associated cancers with physical activity require clarification as a high priority.

References

[1] AICR, Food, Nutrition, Physical Activity, and the Prevention of Cancer: A Global Perspective, World Cancer Research Fund/American Institute for Cancer Research, Washington, DC, 2007.
[2] T. Otani, M. Iwasaki, M. Inoue, S. Tsugane, Body mass index, body height, and subsequent risk of colorectal cancer in middle-aged and elderly Japanese men and women: Japan public health center-based prospective study, Cancer Causes and Control 16 (2005) 839–850.
[3] M. Iwasaki, T. Otani, M. Inoue, T. Sasazuki, S. Tsugane, Body size and risk for breast cancer in relation to estrogen and progesterone receptor status in Japan, Annals of Epidemiology 17 (2007) 304–312.
[4] M. Inoue, N. Kurahashi, M. Iwasaki, Y. Tanaka, M. Mizokami, M. Noda, S. Tsugane, Metabolic factors and subsequent risk of hepatocellular carcinoma by hepatitis virus infection status: a large-scale population-based cohort study of Japanese men and women JPHC Study Cohort II, Cancer Causes and Control 20 (2009) 741–750.
[5] A. Misra, L. Khurana, Obesity and the metabolic syndrome in developing countries, Journal of Clinical Endocrinology and Metabolism 93 (Suppl 1) (2008) S9–30.
[6] B.M. Popkin, L.S. Adair, S.W. Ng, Global nutrition transition and the pandemic of obesity in developing countries, Nutrition Reviews 70 (2012) 3–21.
[7] K.G. Alberti, P.Z. Zimmet, Definition, diagnosis and classification of diabetes mellitus and its complications. Part 1: diagnosis and classification of diabetes mellitus, provisional report of a WHO consultation, Diabetic Medicine 15 (1998) 539–553.